Development of Computer-aided Design Evaluation (CADE) System for Binder Jetting Additive Manufacturing Process from a Manufacturability Perspective

Fan Yang

Department of Mechanical Engineering

Faculty of Engineering

McGill University, Montreal

2017 November

A thesis submitted to McGill University in partial fulfillment of the requirements of the degree of Master of Engineering (Thesis)

Table of Contents

List of figures

List of tables

Abstract

Due to the additive way of manufacturing parts layer by layer, additive manufacturing (AM) is subjected to fewer design constraints than traditional manufacturing techniques. The intricate and complex structures that cannot be fabricated by traditional methods can be realized by AM. However, it should be noted that the manufacturing capability of AM is not limitless. The unprecedented design freedom of AM can only be fully utilized when the unique manufacturability of AM is well investigated and the design methodology specially for AM, also known as design for AM (DFAM), is developed.

One popular topic of the DFAM research is to propose feature-based design guidelines based on experimental investigations. These simple-to-follow rules normally oversimplify the dependent relation between the manufacturability of features and their corresponding manufacturability parameters. To compensate for this shortcoming in the design guidelines, manufacturability analysis is needed to examine designs before manufacturing takes place. In this thesis, a computer-aided design evaluation (CADE) system is proposed to perform manufacturability analysis on computer-aided design (CAD) models for the specific AM process.

The CADE system consists of three consecutive modules: feature detection, feature evaluation and orientation optimization. Logical rule-based method, artificial neural network (ANN) and genetic algorithm (GA) are used to develop the three modules, respectively. A design of experiments (DoE) method is proposed to study the AM manufacturability with respect to selected aspects of geometric dimensioning and tolerancing (GD&T) in a comprehensive yet economical way.

The proposed framework is implemented for the binder jetting additive manufacturing (BJAM) process. Based on the proposed DoE method, the manufacturability of overhang structures and

through holes are investigated experimentally with respect to angularity and cylindricity respectively. The knowledge and experimental data gained in the extensive experimental work are then used to develop the CADE system. With the support of the developed CADE system, designers can examine critical features in their designs from the manufacturability perspective for the specific BJAM process. In this way, the features that are prone to failing are identified in advance so that designers could modify them to decrease the risk of manufacturing failures.

Résumé

De par sa capacité à fabriquer des pièces par couche, la fabrication additive (raccourci en “AM ”, pour Additive Manufacturing en anglais) est soumise à moins de contraintes de conception que les techniques de fabrication traditionnelles. Les structures complexes qui ne peuvent pas être fabriquées par des méthodes traditionnelles peuvent être réalisées par AM. Cependant, il faut noter que les possibilités qu’offre la fabrication additive ne sont pas sans limites. La liberté de conception sans précédent de l’AM ne peut être pleinement utilisée que lorsque ses capacités sont bien étudiées et que la méthodologie de conception spécialement conçue pour l’AM, connue sous le nom de Design for Additive Manufacturing (DFAM), est développé.

Un sujet populaire de la recherche sur DFAM est de développer des lignes directrices de conception basées sur des recherches expérimentales. Ces règles simples simplifient grandement la relation de dépendance entre les possibilités de fabrication et leurs paramètres de fabrication associés. Pour compenser ce raccourci dû à ces méthodes de conception, une analyse de la fabrication est nécessaire pour examiner les designs avant la fabrication. Dans cette thèse, un système d'évaluation de la conception assistée par ordinateur (“CADE ” pour Computer-Aided Design Evaluation en anglais) est proposé afin effectuer une analyse de la fabrication sur des modèles 3D pour le processus AM.

Le système CADE se compose de trois modules consécutifs: la détection des fonctionnalités, l'évaluation des fonctionnalités et l'optimisation de l'orientation. Respectivement, La méthode basée sur les règles logiques, le réseau neuronal artificiel (“ANN ”, Artificial Neural Network) et l'algorithme génétique (“GA”, Genetic Algorithm) sont utilisés pour développer les trois modules. Une méthode de plan d'expériences (“ DoE ”, Design of Experiment) est proposée pour étudier la fabricabilité de l’AM par rapport à certains aspects de la dimension géométrique et du

tolérancement (“GD & T”, Geometric Dimensioning and Tolerancing) de manière globale et économique.

Le cadre proposé est mis en place pour le processus de fabrication additive de dépôt par jet de liants (“ BJAM ”, Binder Jetting Additive Manufacturing). La fabrication de la structure en porte-à-faux et du trou est étudiée par rapport à l'angularité et la cylindricité respectivement. Les connaissances et les données expérimentales obtenues avec ce travail expérimental sont ensuite utilisées pour développer le système CADE. En utilisant le système CADE développé, les concepteurs peuvent examiner les caractéristiques critiques de leurs conceptions du point de vue spécifique de la fabrication par BJAM. De cette façon, les fonctionnalités susceptibles d'être défaillantes sont identifiées à l'avance afin que les concepteurs puissent les modifier pour diminuer le risque de problèmes lors de la fabrication.

Acknowledgements

Foremost, I would like to express my sincere gratitude to my supervisor Prof. Fiona Zhao, who has been nothing but supportive for my Master study and research.

I would also like to take this opportunity to thank all the members of the Additive Design and Manufacturing Laboratory (ADML) in McGill University for their help in any form. Special thanks go to Yunlong Tang, Sheng Yang, Guoying Dong and Zhibo Luo.

My deepest appreciation goes to my parents, who have done everything they can to support me along the way of my abroad life and study. Without their unconditional love and selfless dedication, I could only dream of the life that I have now.

Last but not the least, I really appreciate the financial support of my master study given by Fonds de Recherche du Québec Nature et Technologies – FRQNT team grant 189051.

Contribution of Authors

As required by the Graduate and Postdoctoral Studies in McGill University, the contributions of authors are stated here. The content in Section 3.2.1.1 is published in the proceedings of the ASME 2016 International Mechanical Engineering Congress and Exposition[1]. The co-author of this conference paper, Yunlong Tang, contributed in the content of Section 3.2.1.1.1. Apart from this part of thesis, Fan Yang is the only author of this thesis. Prof. Yaoyao Fiona Zhao is the supervisor and gave important advices in terms of determination of main research orientation, facilities purchase, research method suggestions and paper revision work.

Introduction

1.1 Additive manufacturing

Additive manufacturing (AM), in contrast to subtractive manufacturing that removes excessive material from a workblank to form the desired shape, additively builds parts from scratch by stacking material layer by layer. This manufacturing method has many unique characteristics such as high level of design flexibility[2], low cost of geometric complexity[3] and part consolidation[4] to mention a few. AM processes are categorized in seven types: fused deposition modeling (FDM), powder bed fusion (PBF, including selective laser sintering (SLS), selective laser melting (SLM) and electron beam melting (EBM), etc.), direct energy deposition (DED), sheet lamination (SL), material jetting (MJ), binder jetting (BJ) and stereolithography (SLA). Different AM processes are characterized by some individual process traits, but they all share the same basic principal in general as shown in Figure 1.

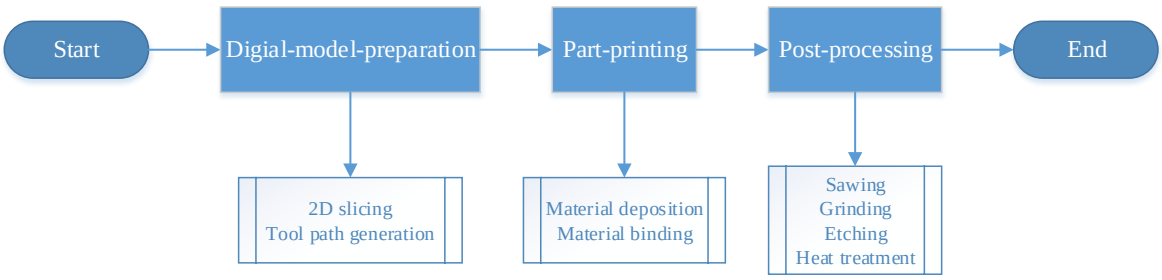

Figure 1. Basic process flow of AM

A typical AM process consists of three basic steps: the digital-model-preparation step, the part-printing step and the post-processing step. The stereolithography file (STL file) is processed by a slicing software in the digital-model-preparation step, where each slice of the as-designed part represents the two-dimensional (2D) shape that will be formed in each layer of the part printing. Since a shaping tool, usually a printhead or a fine beam of energy sources such as laser, electron

beam or ultraviolet light, is normally used to build the sliced 2D shape point by point or line by line, the tool path of the shaping tool needs to be generated by the slicing software as well.

In the part-printing step, each layer of the 2D slicings is constructed by the shaping tool along the designated tool path. Depending on the different kinds of AM processes, different material deposition or material bonding strategies are used. For FDM, EBM and MJ, the shaping material (powder, filament, etc.) is deposited through the shaping tool during the 2D shape construction. As for PBF, BJ and SLA, a layer of shaping material (powder, resin, etc.) is spread from the feed bed to the top of the build bed in advance and then the 2D shape is constructed by the shaping tool that selectively bonds the shaping material on the tool path. The layer-wise repetition of the aforementioned shape-construction process gradually build the desired three-dimensional (3D) shape along the build direction. To remove the excessive material during the part-printing (support structures, build substrate, etc.), or to improve the geometrical quality (surface finish, dimensioning and tolerancing, etc.) and the functional performance (mechanical properties, thermodynamic performance, etc.), further post-processing is usually needed in AM, such as sawing, grinding, etching, heat treatment (sintering, tempering, etc.).

1.2 Manufacturability of AM

The additive way of manufacturing enables AM with unmatched advantages. One of the most game-changing facts of AM is the unprecedented design freedom enabled by the so-called freeform fabrication technique[5]. It was advertised at the time of its advent that AM is free of design constraints because AM can fabricate highly complex shapes and very intricate features. However, with the development and application of AM technology, it became obvious that some unique manufacturing constraints still exist and need to be considered in the design stages[6-9].

The following aspects are some of the typical manufacturing concerns that draw the attention of practitioners.

- Manufacturability of overhang structure: overhang structures whose inclination angle exceeds a certain threshold cannot be formed with satisfying structural integrity[10-13].

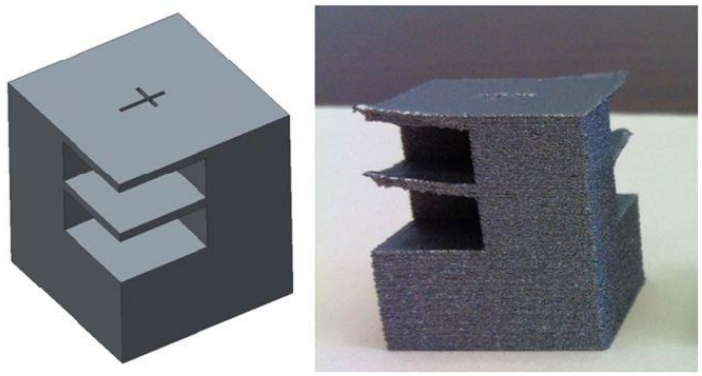

Figure 2. Distortions in an overhang area of an EBAM built part[11]

- Staircase effect: the resolution limitation in the build direction, also known as the staircase effect as shown in Figure 3, leads to a notable geometry deviation between the as-manufactured part and the as-designed model.
- Anisotropy effect: the mechanical properties of AM parts are different along different directions, which makes the build orientation a significant influential factor in terms of the manufacturing limits.

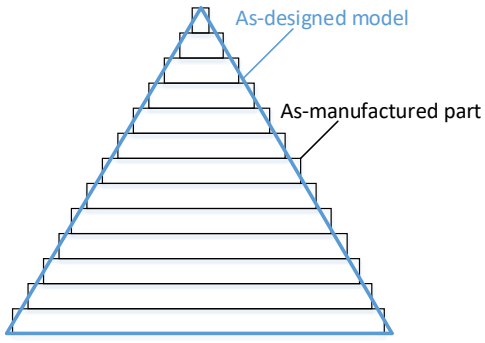

Figure 3. Diagram of staircase effect

These manufacturing concerns are highly linked to whether the selected AM process can successfully manufacture the as-designed parts. Considerations of manufacturability issues in the design stage can help designers reduce the number of design iterations by identifying problematic features in advance. A valid and comprehensive understanding of the manufacturability of any manufacturing process is an important asset and a productive assistance to designers. Nevertheless, AM has only been intensively studied in the recent two decades. Design for AM (DFAM) is specialized for consideration of the unique manufacturing characteristics of AM in the design stage, but the nascent understanding of process characteristics of AM impedes the development of DFAM. More research on manufacturability of AM and DFAM needs to be done to assist practitioners in designing manufacturable parts.

1.3 Literature review of DFAM

Unlike the systematic and well-establish theories of design for manufacturing (DFM) dedicated for traditional manufacturing techniques, the reliable methodologies of DFAM are still under exploration, which leads to this term being used inconsistently in the literature. Kumke[14] wrote an elaborate review on recent DFAM research, in which DFAM is classified in the strict and broad senses. The structure of this DFAM classification is shown in Figure 4. The basic approaches of so-called ‘DFAM in the strict sense’ constitute design rules and methods to ensure AM-producible designs, whereas ‘DFAM in the broad sense’ includes the process selection, upstream activities such as selection of AM parts/applications and downstream activities such as manufacturability analysis. This classification method is used to provide an overview of previous DFAM research while pinpointing the research contribution of this thesis in this given context.

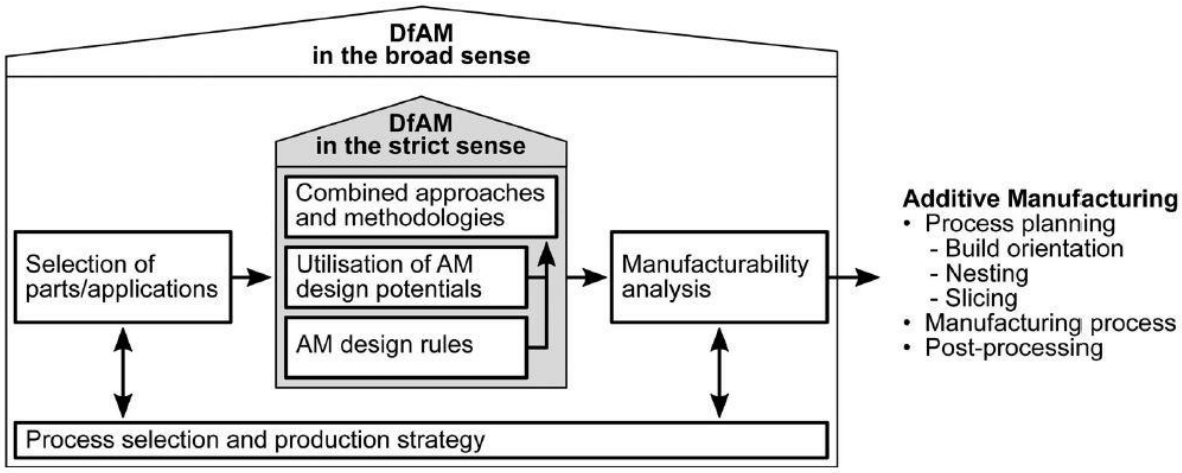

Figure 4. Classification of previous DFAM approaches[14]

1.3.1 DFAM in the strict sense

Concerning the manufacturability of AM, there are two main points of view about DFAM. Most researchers focused on proposing design rules that are related to manufacturing limitations to provide designers with pragmatic guidelines. This is also known as 'the restrictive method'[15]. Thomas[13] evaluated the geometric limitations of SLM based on quantitative experiments and creates feature-based design rules. Seepersad et al.[16] proposed a designer's guide for dimensioning and tolerancing of SLS parts based on the results of a series of experiments[17]. Meisel et al.[18] identified key variables, established relationships between them and quantified design thresholds to create a preliminary DFAM guidelines for the material jetting process. Studies were also done to integrate the design potentials and the unique capabilities of AM in the initial design stage. This is also known as 'the opportunistic method'[15]. Ideal as it may be, limited understanding of AM processes impedes the effective and systematic use of this method. This method primarily focuses on demonstrating through case studies that how existing designs can benefit from AM potentials.

With opportunistic or restrictive methods, practitioners can either focus on the great potential of AM in the preliminary design stage or follow the design rules in the detailed design stage. To

develop comprehensive DFAM methodologies, some researchers combined the restrictive and opportunistic methods in their approaches. Two kinds of approaches are commonly adopted: the bottom-up approach in which no former designs are taken as references in the development of new designs; the top-down approach in which existing designs designed for traditional manufacturing are redesigned and adapted for AM. Goguelin et al.[6] formulated a bottom-up design framework for a new type of CAD tool to support AM. A feature-based design evaluation method was proposed by Ranjan et al.[7] in a graph-based approach from the viewpoint of manufacturability. To benefit from both approaches, Salonitis[19] developed a comprehensive framework of DFAM based on the axiomatic design method that can be used both for developing new products and redesigning existing products.

Apart from the design activities included in DFAM in the strict sense, those that help the DFAM process extend to a broader scope and connect better with the manufacturing process by considering more detailed and comprehensive AM potentials and limitations, also known as DFAM in the broad sense, are far from trivial. A short summary of DFAM in the broad sense is introduced in the next section by emphasising the advantages that it brings to the overall DFAM framework. The research scope of this thesis is also addressed.

1.3.2 DFAM in the broad sense

In the broad sense, DFAM contains additional approaches to providing designers with additional assistance[14]. This category of DFAM contains three main aspects: selection of AM-suitable parts/application, manufacturability analysis and process selection and production strategy, as shown in Figure 4. Among all three aspects, the process selection was investigated the most. Samperi [12] generated a series of design guidelines for metal AM and created a process and machine selection tool. Chen[20] developed an intelligent parameters recommendation system to

predict end-product quality properties and printing time. As for the part selection, Conner[2] et al. identified three key attributes that make a product AM-suitable from a manufacturability perspective. Klahn et al.[21] proposed four selection criteria for replacing conventional parts of a product with additive manufactured ones by re-designing.

1.3.2.1 Manufacturability analysis

Compared with the process and part selections, the manufacturability analysis has not been well studied. Studies on manufacturability are mostly dedicated to guide designers in the detailed design process to create AM-producible parts, as mentioned in Section 1.3.1. However, such manufacturability consideration is normally expressed in the form of feature-based design guidelines. They are sometimes too general to represent the dependent relation between the geometrical aspects of the feature and its potential to be successfully manufactured. To be more specific, design guidelines regarding the manufacturability of AM are normally proposed as recommendations indicating what should be adopted and avoided in the detailed design stage. These guidelines are meant to be simple for the designers to follow, thus they are usually dependant on only one parameter. For example, the guideline of designing overhang structures for SLM is often given as a limitation value of the inclination angle with respect to the build orientation. However, the structural integrity of overhangs highly depends on many other factors, such as dimensions, shapes, topology, etc. Over-simplification of the complex dependent relation will result in the invalidity of the proposed guidelines under certain circumstances. Therefore, it is obvious that the generalized design guidelines cannot guarantee the manufacturability of the design. To compensate for this shortcoming of general design guidelines, manufacturability analysis is needed to examine the generated designs and decrease the risk of manufacturing failures. Manufacturability analysis examines problematic areas of a design with respect to multiple design factors and assessing these areas in terms of manufacturability. In this sense, manufacturability

analysis can be treated as a complementary tool of general design guidelines, that is the manufacturability evaluation of design models in a comprehensive way.

There is a lack of research on manufacturability analysis in the broad sense of DFAM. Among the few relevant research papers, Kerbrat et al.[22] develop a manufacturability evaluation method for the hybrid manufacturing techniques of additive and subtractive processes and implement it in a CAD software, which is not fully focused on AM processes. Zhang et al.[23] propose a two-level evaluation framework for design assessment from a process planning perspective. This research work is dedicated to assessing the parts that are especially designed for AM from a manufacturability perspective. A systematic framework is presented to implement the manufacturability analysis by developing a feature-based computer-aided design evaluation (CADE) system. To assist the implementation of the CADE system, a DoE method is proposed to study the manufacturability of designated AM process. The theoretical and experimental methodologies are elaborated in Chapter 2. The proposed CADE system that is implemented for binder jetting additive manufacturing (BJAM) process is demonstrated in Chapter 3 and a case study of an aerospace bracket is introduced in Chapter 4 to exam the effectiveness of the developed CADE system.

2 Methodology

In this chapter, the framework of a computer-aided design evaluation (CADE) system is proposed to perform manufacturability analysis on digital design models for AM technologies. A generic design of experiments (DoE) method to investigate the manufacturability of the designated AM process is also proposed in this chapter. Involved concepts and terminologies are clarified for the convenience of the following illustrations. The relationship between the DoE method and the CADE system is then introduced, which is followed by the detailed discussions of the DOE method and the CADE system.

2.1 Concepts and terminologies

As a vital link that closely connects the design process with the manufacturing process, manufacturability analysis includes the concepts and terminologies of both design and manufacturing processes. The use of these terms can be inconsistent, interchangeable and confusing. To clarify the context of this thesis, important concepts and terms are defined and illustrated first.

2.1.1 Manufacturability

The concept of 'manufacturability' is not well defined and has been used inconsistently in the literature and in practice. In most cases, it refers to the fact that the part can or cannot be manufactured by the designated manufacturing process. It is a binary indicator of structural integrity, a.k.a. a binary manufacturability. Binary manufacturability is the most fundamental definition. It is a crucial part of the definition and the most basic requirement of the manufacturability of the specific AM process in terms of features, a.k.a. 'the AM feature manufacturability'. However, the binary manufacturability is not very useful in practice. A severely deformed but unbroken feature is indicated as 'acceptable' in the binary definition, however, it is not qualified to fulfill its functionality. In this thesis, 'manufacturability' refers to

the capability of the given AM process to not only successfully manufacture the part, but also ensure that certain design requirements of the manufactured part are satisfied. The proper criteria that reflects the satisfaction of design requirements need to be selected to evaluate the manufacturability.

The determined design is assigned with geometric dimensioning and tolerancing (GD&T) in the detailed design stage. GD&T describes the allowable variation between the nominal (theoretically perfect) geometry of parts and the actual manufactured parts in terms of form and size. The concept of GD&T directly reflects the lowest level of geometric variation that can be redeemed as acceptable. The proper choices of GD&T can directly reflect the main design intentions and design requirements that designers have on the corresponding features, which makes it a perfect match for the manufacturability analysis in the context of this thesis. It is recommended by the author that one or several aspects of GD&T should be chosen as the evaluation criteria of the AM feature manufacturability. It should be noted that the choice of GD&T to be the evaluation criterion can be different for the same feature under different design contexts. Therefore, the evaluation criteria need to be chosen with extra cautions and rational thoughts. For example, for overhang structures, angularity should be selected if both its inclination angle and flatness are the main concerns, whereas other GD&Ts such as roughness or specific dimensions should be selected if they are of more importance otherwise. In this way, the evaluation criterion of the manufacturability of the feature will be chosen as the most important GD&T requirements on that feature.

To summarize, the manufacturability is defined in this thesis as the abilities of the specified AM process to manufacture the part with satisfying GD&T qualities.

2.1.2 Feature

To explore manufacturing limitations of certain AM processes, features have been commonly used as the research objects of DFAM in literatures[13, 16, 24, 25]. Features are generally used to give meaning to component attributes, helping in dissecting component geometry into recognisable, meaningful regions, and improving communication between design and manufacture[26]. In these literature papers, the selected features were experimentally studied, benchmarked and finally summarized as general design guidelines. To stay consistent with the design guidelines being used in the DFAM in the strict sense, features are chosen in this research project as the research objects of manufacturability analysis.

The concept of feature can include but not limited to: design features, manufacturing features, assembly features, measurement features, etc. In this thesis, 'design features' refer to geometric entities that carry the design intentions, such as slot, rib and hole, etc. The set of parameters that determines the geometrical shape of the design feature is called 'design parameters'. For example, a straight through hole is a design feature whose design parameters include diameter and length. 'Manufacturing feature', on the other hand, is determined by both its geometrical shape and the auxiliary non-geometric manufacturing information associated to the manufacturing stage, such as certain process parameters, the process type, material and machine type etc. For instance, build orientation of AM parts is determined by inclination angles, which are process parameters. The rib feature that is manufactured at certain inclination angles is called 'overhang structure', which is a manufacturing feature. To simplify the use of terms in the rest of this thesis, 'features' refer to the features involved in the manufacturability analysis, which can be design features or manufacturing features. Correspondingly, the design parameters and/or non-geometric manufacturing information that have influences on the AM feature manufacturability are called 'manufacturability parameters'.

2.2 Relation between the DoE method and the CADE system

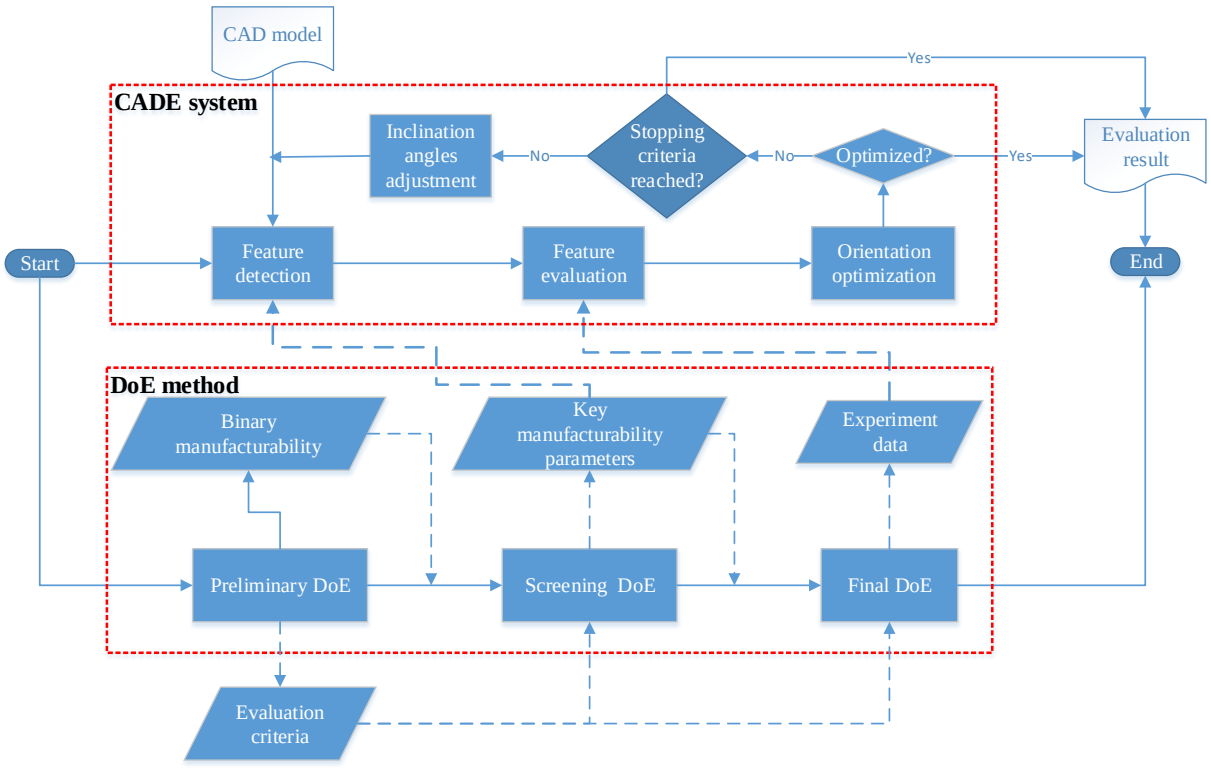

Figure 5. Outline of the DoE method and the CADE system

The CADE system is a computer-aided tool that analyzes the manufacturability of digital design models. Due to the trend of digitization in industry and the inherent advantages of AM in the design and manufacturing automation, computer-aided design (CAD) models are used as the input of the CADE system.

The CADE system consists of three modules as shown in Figure 5: feature detection, feature evaluation and orientation optimization. The first two modules detect and then evaluate the input CAD model for potential features that may have manufacturability issues. However, it should also be noted that one of the most important characteristics of AM is the anisotropic properties of AM parts. The build orientation plays an important role in determining the manufacturability of AM parts. Additively manufactured parts that have a low level of manufacturability under one build

orientation may have a high level of manufacturability under the other, which makes the build orientation an important manufacturability parameter of AM parts. To find the best AM feature manufacturability, the orientation optimization module is needed after the feature evaluation module, as shown in Figure 5. The evaluated result is optimized with respect to the orientation angles. The optimized result predicts the best overall manufacturability of the evaluated CAD model that contains all evaluated features, which is exported into a reference document to designers as the evaluation report. In this study, both the design parameters and the build orientation of features are chosen as the manufacturability parameters.

For the feature detection module, the detection of features should also include the extraction of their manufacturability parameters. For the feature evaluation module, the model of dependent relation between the key manufacturability parameters and the manufacturability of the corresponding feature, that is 'the manufacturability model', needs to be established. The embodiment of these two modules requires the experimental understanding of the AM feature manufacturability and there are two main concerns of the experimentation work. On one hand, the number of manufacturability parameters of each feature can be numerous, especially when the complexity of the feature increases. It is neither efficient nor effective to consider all the manufacturability parameters in the feature detection and evaluation processes. Only the manufacturability parameters that are most important to the manufacturability results, i.e. the key manufacturability parameters, should be used. Thus, it is necessary to identify the key manufacturability parameters of each feature in an experimental way, hence there is the Screening DoE shown in Figure 5. The CADE system only extracts the key manufacturability parameters of the detected features in the feature detection module. The manufacturability parameters that are deemed as relatively unimportant in the screening DoE are neglected and kept as constants in the

subsequent experimental exploration. On the other hand, data acquisition is very important for building the experiment-based manufacturability model. Experimental data pairs of the key manufacturability parameters and the AM feature manufacturability need to be gathered through the DoE method, hence there is the final DoE shown in Figure 5. The final DoE experimentally reveal the influences that key manufacturability parameters have on the resulting manufacturability outcomes. Experimental data is then fed in the CADE system for modeling, which is the feature evaluation module shown in Figure 5.

To sum up, the screening DoE identifies the key manufacturability parameters to save the efforts of feature detection and the final DoE collects experiment data for building the manufacturability model. The three modules of the CADE system are the core of the manufacturability analysis of AM, whereas the DoE method serves as the entry for the CADE system to acquire the knowledge of AM feature manufacturability and experiment data. In this way, the CADE system can be developed based on the experimental understanding of the specific AM process. With the connection between the CADE system and the DoE method being clarified, the following content of this chapter is dedicated to demonstrate them separately. Section 2.4 introduces the DoE method to investigate the AM feature manufacturability and Section 2.3 illustrates the framework of the CADE system.

2.3 Framework of the CADE system

The overview of the framework of the proposed CADE system is introduced first, followed by the introductions of three modules of the CADE system. Although the implementation in Chapter 3 puts emphasis on the BJAM process, the framework proposed in this chapter is a general guideline of manufacturability analysis that can be applied to any features fabricated by any AM processes. Implementation details are different for different situations but the background knowledge of each

module is introduced here. Besides, based on the comparisons among the most plausible choices from the reviewed literature, the reasons of recommending specific methods and algorithms for the implementation are explained.

2.3.1 Modules of the CADE system

Methods and algorithms for the CADE system shown in Figure 6 include: the logical rule-based method for feature detection, artificial neural network (ANN) for feature evaluation and genetic algorithm (GA) for orientation optimization. In the feature detection module, features that will potentially fail to be fabricated in the manufacturing stage are detected via a logical rule-based method. Key manufacturability parameters of detected features are also extracted for feature evaluation. ANN, a type of popular metamodeling method, is used to establish the manufacturability model in the feature evaluation module. The detected features are then evaluated in terms of manufacturability by feeding the extracted key manufacturability parameters in the metamodel. Finally, the overall manufacturability of the design is optimized using the GA. The CADE system is introduced module by module as follows.

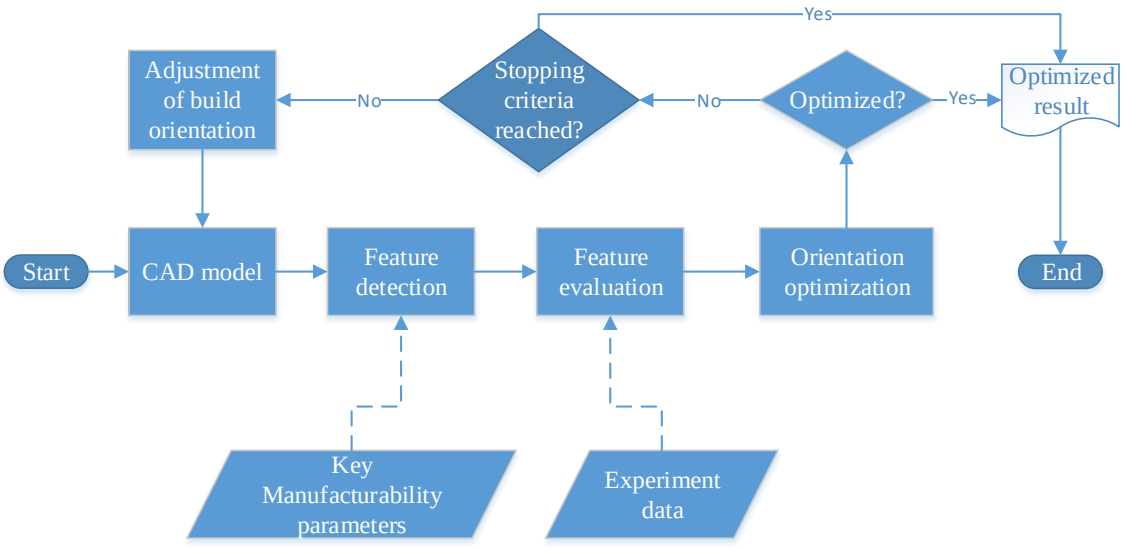

Figure 6. Framework of the CADE system

2.3.2 Feature detection

The feature detection module identifies the potentially problematic features and extracts corresponding key manufacturability parameters for the feature evaluation module. Feature detection is highly linked to the part representation methods employed in the form of CAD data exchange. Boundary representation (B-rep) has most commonly been used in research practice because of easy manipulation of basic elements like vertices, edges, and faces, among which STEP exhibit advantages over other data formats (IGES, ACIS, STL, etc.)[27]. In this framework, CAD models in STEP file format are employed.

The process of detecting features in CAD models and extracting geometric information of these features, more formally known as feature recognition (FR), has been studied for many years. FR is an essential process for fully automated computer-aided process planning (CAPP) system development[27] in traditional manufacturing techniques. Integration of a design system and a manufacturing system by using the concept of features has been a major research direction for many years[26-30]. It is dedicated to converting design feature information in CAD system to the machining feature information in CAM system, during which instructions of how the part should be traditionally manufactured are determined. The existing theories and methods of FR are especially developed for traditional manufacturing and therefore can not be directly used in the context of AM. However, the basic ideas and principles are similar and most of the popular techniques are interlinked. For example, in terms of approaches of FR for traditional manufacturing, logical rule-based method is commonly used in the feature recognition due to it robustness[27]. The features should be exclusively defined so that robust detection logics can be established. The exact detection logic may not be feasible for AM parts but detection algorithms for primitives such as faces, edges and vertices and simple features like holes, slots, chambers, and bosses are applicable in the context of AM with some minor modifications. Attributes of CAD

model such as faces, edges, vertices and their topology information are normally used to identify features and extract geometry information. With a good knowledge of the designated AM process and the existing detection methods of FR, the detection logics and algorithms can be adapted for AM by eliminating unnecessary considerations of traditional techniques (such as the multi-step process planning) and adding special concerns of AM features (such as closed internal cavities). It is suggested in this framework that a logic rule-based feature detection module for STEP files should be developed to identify the features and extract the value of their key manufacturability parameters.

It is crucial to have well-defined features with no ambiguity, which means one type of feature must uniquely correspond to one definition in the entire knowledge base of features and vice versa. The uniqueness of feature definition ensures an accurate recognition if set up correctly. However, given the diversity of feature definitions, it's almost impossible to embrace all possibilities of similar features in one single definition. To benefit from the advantages of a rule-based method while preventing the detection logic from being too lengthy and complicated, it's important to keep the applied range in mind and develop the logic (if-then) rules as efficient as possible in the designated application background. It should be noted that it is surely beneficial to develop a comprehensive feature knowledge base of feature definitions and detection logics, but only the tradeoff between budget and detection performance matters the most. The CADE system should be developed for the features that are most crucial first, and more design features can be incorporated afterwards if more resources are available. In this thesis, the detection logic for overhang structures and through holes are developed and explained in Section 3.3.1.

2.3.3 Feature evaluation

Once the features of interest are detected, the next step of CADE system is to evaluate the detected features and find the best build orientation for the best overall manufacturability of the entire part. The manufacturability model needs to be developed to map the values of key manufacturability parameters into the manufacturing results. The formulation of mathematical models based on physical understanding of AM processes is an important approach to establishing the mapping relation; however, it may be quite a challenging task as it requires in-depth understanding of the complex AM processes[31], which are not available for most metal AM processes at present. Therefore, researchers focus on building empirical models using data-driven metamodeling techniques such as ANN[32-35], response surface method (RSM)[33, 36], regression model[37], statistical modeling[38-40], genetic programming[35], etc. Among all the metamodeling methods, RSM and ANN are two most popular techniques used for the metamodeling of manufacturing processes. RSM is a statistical-based approach in which a response of interest is approximated by fitting the experimental responses to polynomial functions[41]. It is a stepwise heuristic method that often locally uses linear functions to approximate a global response surface with second-order polynomial equation[42]. The number of many successful applications of RSM has proved it to be an effective metamodeling method. On the other hand, ANN has emerged as an attractive tool for non-linear multivariable modeling[43]. ANN is the state-of-the-art approach to exploring complex yet vague relation by giving computers the ability to learn from previous data without being explicitly programmed. Comparatively speaking, ANN has many advantages over RSN in the context of this thesis: (i) ANN is capable of approximating almost all kinds of non-linear functions including quadratic functions, i.e. the universal approximation capability, whereas RSM is useful only for quadratic approximations[41]; (ii) the multilayered structure of ANN has the capability of establishing complicated relationships and it provides the flexibility of fine-tuning the ANN

structure by changing the number of hidden layers and the number of neurons in each hidden layer; (iii) there are plenty of useful diagnostic techniques for training ANN algorithms such as regularization, learning curves, gradient checking, error analysis, etc., which makes ANN an effective and efficient metamodeling method. It is reported in many reviewed literature papers[32, 33, 36, 41, 44-49] that ANN showed a clear superiority over RSM in terms of prediction accuracy, efficiency, data fitting and estimation capabilities. Moreover, ANN has been proven to be effective in modeling many AM processes[33-35, 50-52]. Besides, ANN is suitable when the relationship between the inputs and responses is unknown or there is an incomplete understanding of the process[31], as in the case of most metal AM processes like the BJAM process. Given the advantages of ANN and successful application of ANN in AM processes, ANN is chosen as the metamodeling method of the feature evaluation module.

2.3.4 Orientation optimization

The orientation optimization module determines the best overall manufacturability of the part with respect to the build orientation. The GD&T requirements that are used as the evaluation criteria, such as angularity for overhang structures and cylindricity for through holes, are found to be orientation-dependent for most AM processes. It is a complicated dependent relation that cannot be fully embraced in the design guidelines. Therefore, it is very difficult to manually determine the build orientation that results in the best manufacturing quality when designers come up with the design using the design guidelines. On one hand, the build orientation preassigned by designers can fall outside of the feasible range of orientation angles because of the over-simplification of design guidelines explained in Chapter 0. On the other hand, the build orientation is a crucial part of the definition of some manufacturing features. For instance, a rib structure inclined 90 degrees over the build plate is considered as a vertical-wall feature, whose manufacturability in AM processes is normally not determined by the same set of key manufacturability parameters as those

of overhang structures, thus, should not be detected and evaluated as the same type. Considering the significance of build orientation, an orientation optimization module is integrated in the CADE system, which includes a scheme of orientation adjustment, as shown in Figure 6. The orientation optimization module changes the orientation of the CAD model, so that features are re-detected in the feature detection module and the re-detected features are re-evaluated in the feature evaluation module. The orientation optimization module checks the evaluation results again to continue changing inclination angles if necessary. The looping stops until the optimized result is found or the stopping criteria are reached.

The optimization of build orientation of AM parts is a popular research topic in the research field of AM. It is usually a trade-off between multiple objectives based on many variables of various types (continuous, discrete, categorical, etc.). The characteristics of the resulting objective function are most likely not suitable for traditional optimization algorithms where continuity and/or differentiability are often required. Genetic algorithm (GA), on the other hand, utilizes techniques inspired by evolutionary biology such as inheritance, mutation, selection, and crossover to tackle large-scale optimization problems[53]. GA is suitable to find the global extremum hidden among many poor and local extrema[54], which has been successfully applied to build orientation optimization of AM parts in literatures[34, 53, 55, 56]. Thus, GA is used for the orientation optimization module of the proposed CADE system.

2.4 Framework of the DoE method

A three-stage DoE method is proposed here to guide the practitioners to develop a series of experiment procedures for investigating the AM feature manufacturability. It consists of preliminary, screening and final DoE, whose framework is shown in Figure 7. Except for the screening and final DoE mentioned in Section 2.2, a preliminary DoE is also needed when the

basic manufacturing capacity of the AM process is unclear or the manufacturability of the specific features fabricated by this specific AM process is unknown. Moreover, the evaluation criteria that indicate the satisfaction of certain GD&T requirements need to be selected in the preliminary DoE as well. The evaluation criteria will be inherited from the preliminary DoE to the screening and final DoE shown in Figure 7. To gain the basic understanding of the designated AM process such as the binary manufacturability and select the proper evaluation criteria of manufacturability, the preliminary DoE is employed in the DoE method shown in Figure 7.

In the proposed DoE method, understanding of binary manufacturability and evaluation criteria, key manufacturability parameters as well as experiment data are drawn from three stages of the DoE method to support the next experiment stage. The acquired knowledge and data are then used to establish the CADE system. It should be noted that details of the DoE method might vary for different AM processes, but a general yet systematic methodology is proposed here to guide the experimental exploration for the manufacturability of AM.

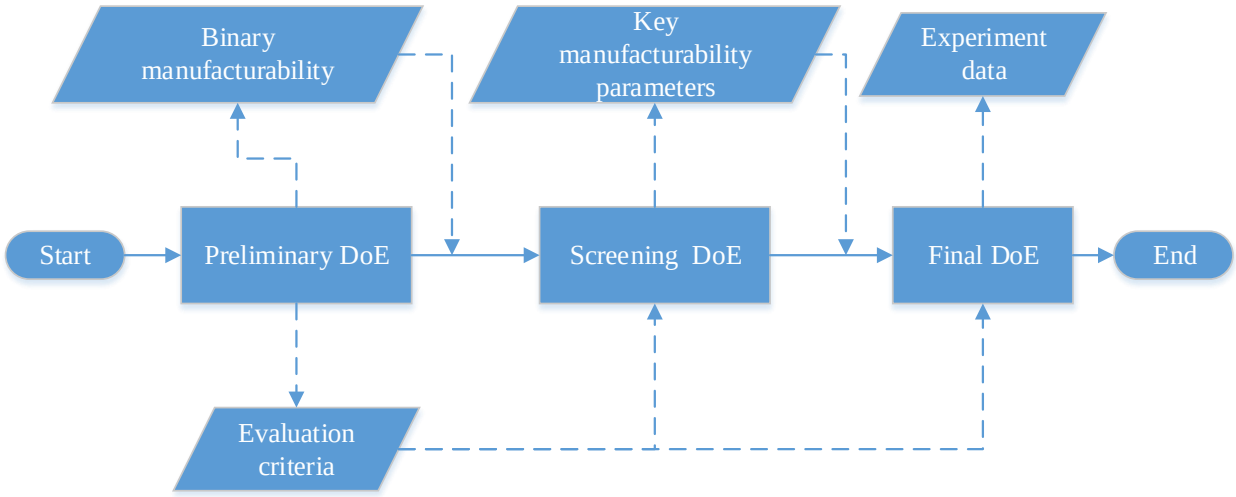

Figure 7. Framework of the DoE method

2.4.1 Preliminary DoE

The preliminary DoE is implemented to understand the binary manufacturability of the designated AM process and select the proper evaluation criteria of its feature manufacturability. It is almost impossible to propose a specific method for the preliminary DoE because it can be dramatically different for various AM processes and for different features of interest. For example, the depowdering process is crucial for the manufacturability of BJAM process, whereas it is not very important for the laser-based metal AM processes since the dense parts are already solidified. The difficulty of depowdering overhang structures is that the structure is too fragile, whereas the difficulty of depowering through holes is that the inner surface is hard to reach. Therefore, details of the preliminary DoE need to be determined by considering the characteristics of the specific AM process and the evaluated features. As mentioned in Section 2.1.1, the most basic requirement of the AM feature manufacturability is the binary manufacturability. A set of experiment samples should be designed by changing manufacturability parameters so that some initial conclusion of the binary manufacturability can be drawn. Since the initial selection of manufacturability parameters, evaluation criteria and measurement method and equipment may not be suitable, some iterations might be needed. At the end of preliminary DoE, the GD&T requirements chosen as the evaluation criteria need to be determined. Given experiment conditions and the budget of time and money, the corresponding measurement method and equipment also should be specified.

The preliminary DoE is the initial exploration of the AM feature manufacturability and a preparation step for the following stages of DoE. It should be noted that the preliminary DoE is not mandatory but highly recommended.

2.4.2 Screening DoE

A screening scheme is needed to identify the key manufacturability parameters. Screening DoE is the most popular form of fractional factorial DoE used to reduce the number of process or design parameters (or factors). It identifies the key parameters that affect process performance or product quality[57]. Especially when a system or process is new, it efficiently seeks out the non-influential factors to remove from experimentation[58]. Screening designs are a practical compromise between cost and information by making the assumption that the process in the real world is dominated by only a few factors whereas the rest being relatively unimportant[59].

Traditional screening DoE pinpoints the factors that have dominant effects by assuming a linear effect of factors on response in the applied process or system. Substantial ambiguity will be presented if a nonlinear or confounded effect is active. Confounding occurs in many standard screening designs with a similar number of runs. Traditional screening DoE such as resolution III or IV designs cannot capture curvature due to pure-quadratic effects[60]. Subsequent experiments are needed to analyse the active interactions.

To tackle this issue, definitive screening design (DSD) was recently introduced by Jones and Nachtsheim[60]. DSD is suitable to identify the main effects and second-order terms in one stage of experimentation[61]. DSD only requires a small number of runs to not only detect the important factors and interactions but also identify the cause of nonlinear effects. It efficiently provides the feature detection module in the CADE system with unbiased information. Moreover, the identification of correlated factors is very important for the selection of experiment method for the final DoE. Taguchi method is recommended for the final DoE, which is introduced in the following section, but the presence of interactions among factors can cause the estimate of performance by Taguchi method to be significantly off[33]. DSD can test the suitability of Taguchi method for the final DoE.

To screen out unimportant factors and guide the method selection of final DoE, DSD is employed to identify key manufacturability parameters and exam potential interactions between them. There are many ways of developing a DSD, among which the most popular choice is to use the DoE platform in the modern statistical software like JMP and Minitab. It is convenient to make an experiment design and analyze the experiment results in the same place. A good DoE platform offers both robustness and flexibility and practitioners can have their own choice of DoE platform to develop the DSD runs. In this thesis, JMP created by the Statistical Analysis System (SAS) is used in Chapter 3 to implement the proposed screening DoE.

2.4.3 Final DoE

The final step of the proposed three-stage DoE method provides experiment data for ANN to learn from. As mentioned in Section 2.4.2, Taguchi method is the recommended DoE method. It is a robust, efficient and cost-effective DoE method that is widely used in developing a product or investigating a complex process in industry. It requires a small number of experiment runs while providing fruitful information of the investigated product or process. Taguchi method provides an effective means to enhance the performance of ANN in terms of the learning speed and the recall accuracy[32]. Regarding the data mining of ANN, Taguchi method was found to be an effective means to enhance the performance of ANN in terms of learning speed and accuracy[62]. ANN that is built on the experiment data designed by Taguchi method provide a good prediction in a variety of physical processes[62-64]. Another advantage of employing the Taguchi method is that the structure and parameter tuning of ANN by using Taguchi method and GA can reduce the cost of implementation of ANN[65]. It is shown in the literature[35, 62, 65] that ANN, GA and Taguchi method work well with each other and the combination of them is an effective and efficient approach to optimizing and modeling nonlinear and multitudinous systems[35]. Therefore, it is suggested to use Taguchi method for final DoE.

Taguchi method is a preferable choice of the final DoE but its suitability is highly dependent on the information acquired in the screening DoE and the characteristics of ANN structures. The possible presence of factor interactions detected in the screening design may disagree with this choice. In this case, other fractional factorial DoE, such as central composite design, Latin Hypercube design and other designs supplemented with domain knowledge should be used. Therefore, the specific DoE method for the final DoE cannot be determined before the analysis result of the screening DoE is gained.

2.5 Summary

Design guidelines used for designing parts especially for AM are typically oversimplified. The satisfaction of all guidelines does not guarantee the successful manufacture of the as-designed part. Manufacturing analysis, in which the design model is examined for potential manufacturing failures, is needed to save the money and time of product development for AM.

To provide practitioners with a convenient yet effective approach to performing manufacturability analysis on AM parts, the framework of developing a computer-aided design evaluation (CADE) system in an experimental way is proposed in this chapter. For the designated AM process, its feature manufacturability is first studied experimentally by following a series of DoE procedures. A three-stage DoE method is introduced to provide essential information and data for the CADE system. The preliminary DoE acquires the most basic understanding of the AM feature manufacturability, that is the binary manufacturability. The screening DoE identifies the key manufacturability parameters to relieve the workload of subsequent experiments. The final DoE supplies experiment data on which the manufacturability model of feature evaluation is built. The results and analysis of systematically designed experiments are then used to assist the development of the CADE system.

The proposed CADE system is characteristic of being a computer-aided and feature-based software tool. Given the traits of the CADE system and the anisotropy of AM parts, three constituent modules of CADE system are embodied with carefully selected methods and algorithms: the logical rule-based method for feature detection, artificial neural network (ANN) for feature evaluation and genetic algorithm (GA) for orientation optimization. The combination of Taguchi method, ANN and GA is recommended for the data acquisition and development of CADE system. The CADE system takes the CAD model as the input to generate the manufacturability evaluation result of potentially problematic features. In this way, potential manufacturing issues can be identified before the actual manufacturing process.

However, it should be noted that this proposed approach is subjected to some limitations that need to be tackled. For one thing, the logic rule-based method used for feature detection is favored for its robustness. However, this kind of one-to-one mapping in the feature database is lack of knowledge acquisition and update mechanism[10], therefore continuous update work is needed whenever there is some change of the feature detection logic or a new feature to be added. Besides, serious issues can be caused when the detected features cannot find any match-up pattern in the knowledge base. For another, ANN is an advanced algorithm that does not need explicit programming and thus the mapping relation is not established in an explicit form. The ANN model cannot explain the results explicitly, which implies that the question of how the design should be modified for improvement is out of the scope of this thesis.

3 Implementation of the DoE methods and the CADE system for BJAM

In this chapter, the DoE method and the framework of the CADE system proposed in Chapter 2 are implemented for binder jetting AM (BJAM) process.

3.1 BJAM process

Binder jetting, also known as three dimensional printing (3DP), is a direct digital fabrication technology that selectively deposits a liquid binder into a bed of loose powder to form a green part whose shape is given by CAD specifications[66]. The printing system of BJAM is shown in Figure 8. The spreading roller spreads a thin layer of powder over the powder bed in the build box, then the binder in the liquid binder supply is applied to the powder bed through the inkjet printhead to form a 2D shape and bonds it with the one in the previous layer. After the deposited binder is solidified by an electrical infrared heater, the powder supply in the feed box is moved up and the build box moves downwards by one layer, so that a new layer of powder can be spread. The aforementioned process repeats which gradually forms a 3D printed part, a.k.a. the green part. This green part, still embedded in the powder bed, is transferred into a curing oven to solidify the liquid binder. This process is called the curing or debinding process. The green part is imposed with enough strength for the following operations. The loose powder around the green part is removed in the depowdering process. The sintering/infiltration burns off the solidified binder and allows the formation of inter-particle necks that add strength to the part while minimizing dimensional changes[67]. The part formed after the sintering/infiltration process is called a brown part, and it is further post-processed by operations such as polishing to form a final part if necessary. It should be noted that “green” and “brown” parts used here are characteristic idioms borrowed from Laser Sintering (LS) process. In LS process, material powders are fused and bonded to form a porous green part, then a stronger brown part is formed after the sintering process removes internal pores

of the green part. It shares a certain similarity with BJAM in this sense, thus a ‘green part’ refers to the weak and porous part after the depowdering process and a ‘brown part’ refers to the sintered part after the sintering process. The aforementioned processes are summarized in Figure 9.

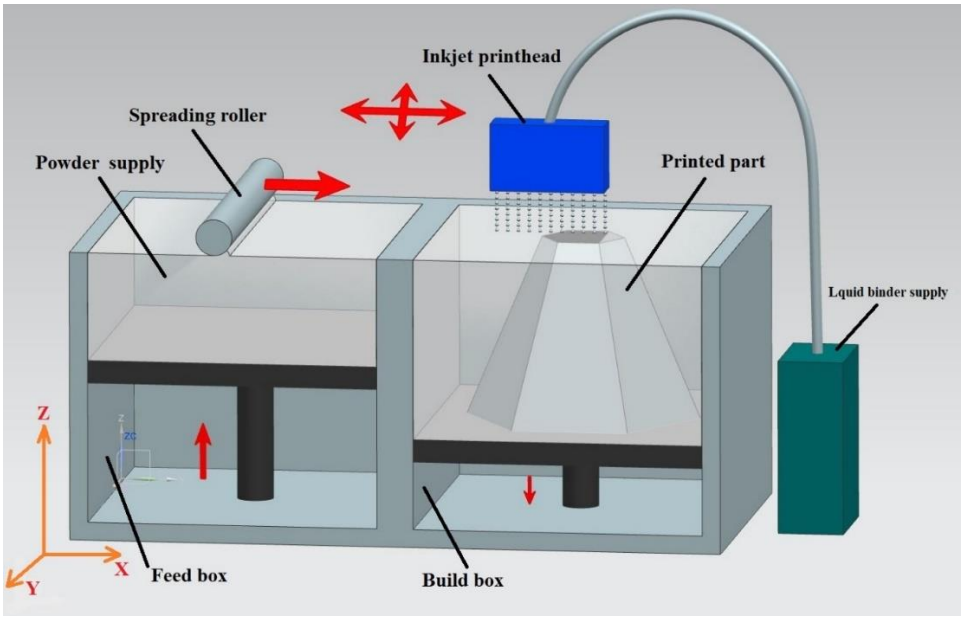

Figure 8. Diagram of the printing system of BJAM

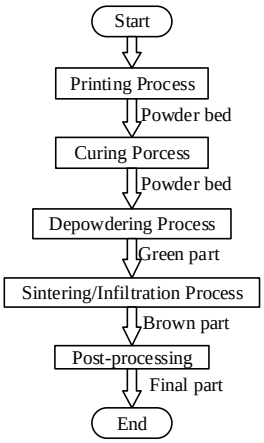

Figure 9. Flowchart of the BJAM process

Compared to other metal AM processes, there is no intensive heat input in BJ printing process. Moreover, the loose powder which acts as support structures for overhangs during the printing

process can be easily removed after the curing process. These advantages of BJ make it suitable for fabricating overhang structures[67]. The manufacturability of laser-based metal AM are relatively intensively investigated as mentioned in Section 1.3. BJAM process, on the other hand, is filled with many unknown questions. To cope with this issue, the CADE system is developed especially for the BJAM process. Due to the need of experimental analysis and data for the implementation of the CADE system, the experimental work is introduced first.

3.2 Design of experiments

The three-stage DoE method proposed in Chapter 2 is implemented here for two features that are critical for AM processes: overhang structure and through hole, as shown in Figure 10. These two types of design features are commonly known for their low level of manufacturability in AM. Overhang structures normally require the support structure to avoid deformation caused by the thermal stress when intensive heat input presented. Attentions is also required for designing through holes since there is the minimum size of manufacturable through hole and the quality of through holes varies significantly under different orientations. The experimental work for these two features are illustrated separately.

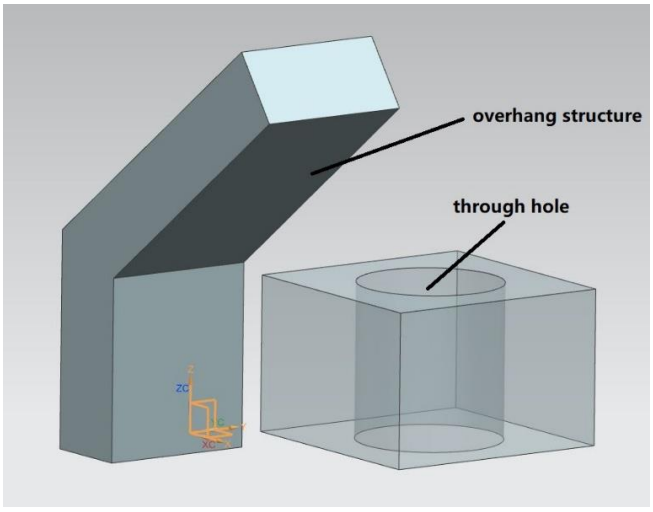

Figure 10. Diagrams of overhang structure and through hole

3.2.1 Overhang structure

Due to the lack of research in the literature, preliminary experiments are conducted to investigate the manufacturability of overhang structures fabricated by the BJAM.

3.2.1.1 Preliminary experiments on overhang structures

Protruding features are commonly used in mechanical parts such as connectors, brackets, etc. As for the fabrication of these features via AM processes, sometimes they are unavoidably manufactured as overhang structures due to the limited printing space or due to a specific printing orientation resulting from other limitations. In the context of AM in this thesis, an overhang structure is defined as a type of manufacturing feature that needs additional support material during the fabrication process. Compared to other metal AM processes, BJAM have advantages of no severe temperature variation during manufacturing and easy removal of loose powder which act as support structures during the printing and curing process. However, like other AM processes, it should be noticed that the BJAM process also has certain manufacturing limitations on overhang structures. It is crucial to have a general idea of the manufacturability of the BJAM process before implementing the CADE system. To deal with this issue and provide a general guideline for designers, the binary manufacturability of overhang structures fabricated by BJAM is studied both experimentally and theoretically. A theoretical model is proposed to predict the fracture failure of overhang structures in the depowdering process and proper experiments are designed to validate the proposed model. The methodology and experiment research are explained as follows. The content of Section 3.2.1.1 is published in the proceedings of the ASME 2016 International Mechanical Engineering Congress and Exposition[1].

3.2.1.1.1 Theoretical model for the depowdering process

The depowdering process is a unique manufacturing step of BJAM process. On one hand, the material powder particles are only loosely connected by solidified binder as shown in Figure 11.

Therefore, compared to the brown part after the sintering process, the strength of green part is relatively weak and vulnerable to fracture. On the other hand, the green parts lose the support of extra loose powder after the depowdering process, which could easily be damaged by some inevitable external loads, such as self-weight. Based on the past experience, fragile structures like overhang structures tend to fail during the depowdering process. A theoretical model is proposed to predict the fracture failure of overhang structures during the depowdering process of BJAM. This theoretical model mainly focuses on the fracture of green parts obtained after the depowdering process.

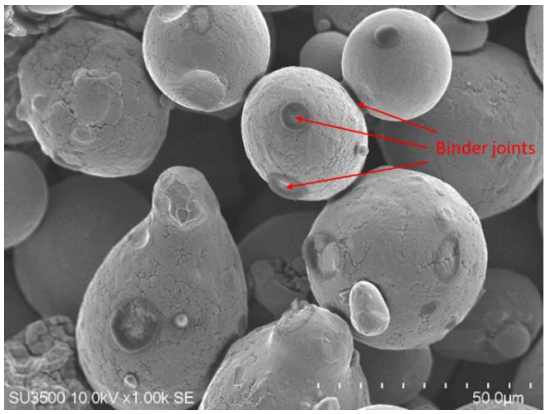

Figure 11. SEM of the fracture cross section of green part

Based on the observation of broken green parts during the depowdering process, it is seen that these parts usually fail without any extensive plastic deformation. Thus, the failure of green parts after the curing process can be classified into brittle failure category. To predict the failure of green parts, the maximum normal stress criterion is used. According to this theory, the failure occurs when the maximum principle stress reaches to the uniaxial tension strength. It can be expressed as:

$$\sigma_m < \sigma_t \quad (1)$$

Where σ_t is the uniaxial tension strength of the printed green part. It can be assumed as a constant if certain material and binder as well as the processing parameters are selected. σ_m is the maximum

principle stress of the specimen after the depowdering process. The stress inside the green part during the depowdering process is mainly caused by its self-weight as well as any forces imposed by the operations such as brushing, air-blowing and/or vacuuming. The depowdering forces are highly related to depowdering strategies being used and the operation skills. Despite the nature of randomness of depowdering forces, experienced operators can successfully use proper strategies to avoid fracture failure caused by depowdering forces. For example, a sudden extraction of loose powder support to the overhang structures should be avoided, thus the loose powder above the upward surface of overhang structures should be removed first while the downward surface is supported. In order to explore the dimensional requirements that designers must obey to ensure the structural integrity of overhang structures, the depowdering forces are neglected and focus is given on the determination of the limit stress condition solely caused by self-weight. In other words, the designed overhang structure must be a self-supporting structure. Figure 12 shows one of the most common overhang structures that occur during AM processes. According to beam theory, the maximum normal stress for the structure shown in Figure 12 is located at the point A or B. This value for any arbitrary shape can be calculated by equation (2):

$$\sigma_m = \frac{M \cdot z}{I_z} \tag{2}$$

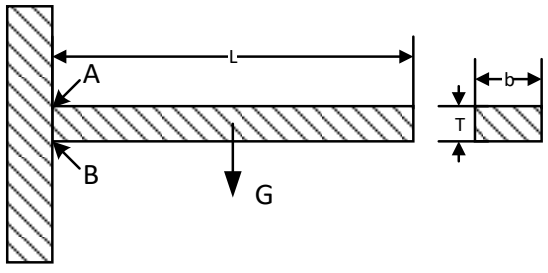

Figure 12. Example of typical overhang structures

Where M represents the bending moment at the point A or B; z is the maximum distance between point A/B and the neutral axis of the beam, and I_z is the area moment of inertia of the cross-section.

$$M \cdot \mathrm{z} = G \cdot (\mathrm{L}/2) \cdot (\mathrm{T}/2) \quad (3)$$

$$G = \rho \cdot bTL \cdot g \quad (4)$$

$$I_z = \frac{\mathrm{b}T^3}{12} \quad (5)$$

$$\sigma_m = \frac{3\rho g L^2}{T} \quad (6)$$

The geometrical relations of a rectangular beam are listed above, where G represents the self-weight of overhang region; ρ is the density of green part; g is gravitational acceleration; b, H, L are width, thickness and length of overhang beams, respectively. To avoid the collapse of green parts, σ_m in equation (2) should be minimized and kept lower than σ_t. Designers can change the design parameters of the overhang region to decrease σ_m. From the equations (3) to (5), it can be concluded that both the thickness T and the length L have effects on the maximum normal stress of printed green parts, as shown in equation (6). In the next section, experiments are conducted to explore the limit value of σ_m by altering the design parameters of overhang testing samples, with an emphasis on investigating the fracture failure caused by self-weight of overhangs.

3.2.1.1.2 Experiments and results

Apart from the design parameters of overhang structures as discussed in the previous section, there are many other manufacturability variables that could have an impact on the mechanical performance of green parts. For example, printing and curing process parameters determine the way that liquid binder is deposited and solidified to finally bond powder particles. To explore the maximum value of σ_m caused by self-weight, i.e. σ_t, a set of default parameters of these variables needs to be properly chosen and maintained at the same level throughout the experiments.

The major printing process parameters of the BJAM process, i.e. layer thickness, printing saturation, heater power ratio and drying time, have been studied by Chen et al.[20] and the optimized parameters are given. Given the fact that the overall printing process takes a long time,

the economical optimized parameters as proposed in Chen's research are chosen to be used throughout this research. Moreover, the powder-binder-cleaner material system and the curing parameters used is the default combination as proposed by the equipment supplier—ExOne company. All the experiment specification is shown in Table 1.

Table 1. Experiment specification

Variables	Specification
Powder	S3-30 Powder (30μm 316 Stainless Steel)
Binder	BS003 Solvent Binder 03
Cleaner	CL001 Cleaner
Curing Parameter	5 hours at 175 °C
Layer Thickness	100μm
Printing Saturation Ratio	75%
Heat Power Ratio	70%
Drying Time	30 seconds

Experiments are conducted on ExOne X1-Lab Binder Jetting system[68]. The build volume is 60mm*40mm*30mm (L*W*H), which limits the dimension of parts that can be fabricated. According to ASME E8 standard, the minimum overall length of subsize specimen is 100 mm, which is out of the scope of build volume of this printer. To overcome the difficulty of measuring the tension strength σ_t via mechanical testers, an alternative measurement method is proposed here. The schematic diagram of the testing sample is shown in Figure 13. A rectangular block is added at the tip of overhangs, acting as a weight that loads a concentrated force F on the overhang. The weight block contributes to the increase of the maximum normal stress, which can be controlled by changing the dimensions. The maximum normal stress in Figure 13 can be calculated by equation (7):

$$\sigma_m = \frac{3\rho g L^2}{H} + \frac{6\rho g l\left(L-\frac{l}{2}\right)h}{H^2} \quad (7)$$

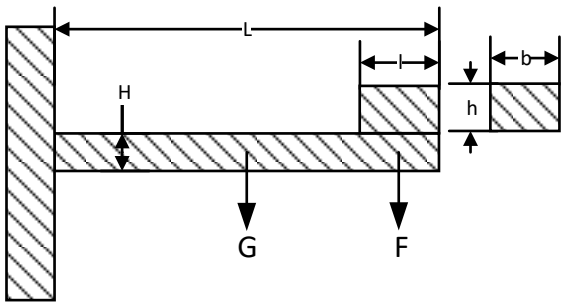

Figure 13. Schematic diagram of the testing sample for σ_t

Where l and h is the length and height of the rectangular block, respectively, and the remaining symbols are the same as in the equations (3) to (6). The first term in equation (7) is the contribution of self-weight of the overhang itself, which is the same as shown in equation (6), while the second term is the contribution of the concentrated load F imposed by the self-weight of the rectangular block at the tip. By having L, T and l fixed and increasing the height of the weight block h, the maximum normal stress σ_m will eventually reach to the value that leads to the fracture failure, i.e. the tensile strength σ_t. The value of σ_t can be calculated by equation (6) and a set of overhang structures are designed to acquire it.

The density ρ of the green part is needed for the calculation of σ_m, as shown in equation (6). Although the green part is very porous, the porosity is fixed for fixed manufacturing parameters and powder-binder-cleaner material system. A set of cubes are printed to estimate the density ρ, and the value is determined to be $4.26\ g/cm^3$. In order to narrow down the value range of tensile strength σ_t, pre-experiments are designed with a set of overhang structures as shown in the left of Figure 14. The normal stresses of these overhangs are designed to discretize the value range of σ_t, and the fracture failure indicates that it falls in the range of 3.5MPa to 5.0MPa. Given the limited dimension of build volume and results of the pre-experiments into consideration, testing samples as shown in Figure 13 are designed. The changing height of weight blocks and the corresponding

normal stresses σ_m are listed in Table 2, while the fixed dimensions are: L = 50 mm, l = 14 mm, H= 0.5 mm. The states of structural integrity are listed in Figure 14, which are also shown to the right of Figure 14. The resulting structural integrity of testing samples indicates that σ_t is in the range of 5.0–5.1MPa, which is limited to the material system, process parameters and the machine being used in this research.

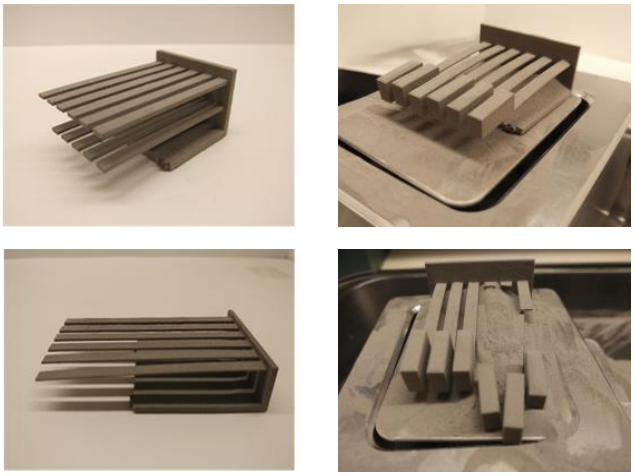

Figure 14. Pictures of testing samples

Table 2. Experiment results of structural integrity

h (mm)	σ_m (Mpa)	Structural Integrity (X---fractured, O---unfractured)
5.0	3.64	O
5.2	3.76	O
5.3	3.82	O
5.5	3.94	O
5.7	4.06	O
5.9	4.18	O
6.9	4.79	O
7.1	4.91	O
7.3	5.03	O
7.4	5.09	X
7.6	5.21	X
7.8	5.33	X

3.2.1.1.3 Manufacturability parameters and evaluation criterion of overhang structures

The manufacturability parameters include the design parameters (width W, length L and thickness T) and inclination angles α and β shown in Figure 15. The inclination angle α with respect to the X-Y plane is the common manufacturability parameter that is associated with the anisotropy of AM processes, whereas the angle β with respect to the X-Z plane is a special manufacturability parameter for the BJAM process.

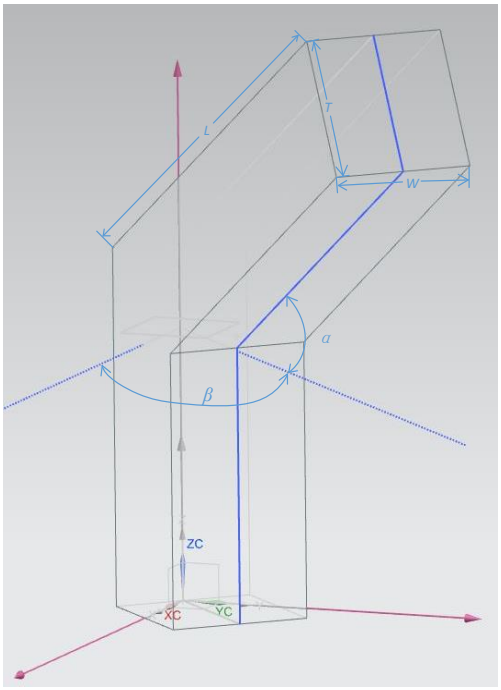

Figure 15.Diagram of the typical overhang structure

It has been noticed by the author that it is common to have a strip texture on the parts along the direction in which the binder droplets are applied(the Y axis in Figure 8), as shown in Figure 16. The overhang structures tend to break along the same direction. This implies a special anisotropic property of parts fabricated by BJAM. To confirm the hypothesis of complex anisotropic properties of BJAM parts, compression and tensile tests are conducted following ASME E9-89a(2000) and ASME E8/E8M-13a Standard Test Method. The sizes of test parts are D13*H25mm cylinders for compression tests and subsized dogbone samples for tensile tests. It should be noted that all test samples are only sintered without infiltration of bronze, which is the main cause of the poor mechanical performance. The default sintering profile suggested by ExOne is listed in Figure 17. Printing and curing process parameters listed in Table 1 and the default sintering profile are used throughout the experiment exploration of the manufacturability of BJAM process. The test results in Table 3 show that there is a big difference among parts printed in different orientations in X-Y plane. It can be concluded that BJAM process not only suffers from

the anisotropic effect in the printing direction as any other AM processes do, but are also subjected to the anisotropic effect in the direction in which the binder droplets are applied. Mechanical properties are highly influenced by this complex anisotropic effect of BJAM, which can be very detrimental to the manufacturability of fabricated parts. Therefore, in the context of BJAM, there are five manufacturability parameters important to overhang structures: width W, length L, thickness T, and inclination angles α and β.

Based on the observation that a small deflection of typical overhang structures in Figure 14 will lead to the fracture at the root, angularity is a great choice of evaluation criterion. Angularity is a great combination of measuring both the flatness tolerance of the overall structure form and its angle dimension. In the following screening DoE, five manufacturability parameters are studied in terms of their relative importance of influence on the angularity of overhang structures. Confounding effects and the corresponding causes, if any, are identified to guide the method selection of final experiments.

Considering the fragility of some samples with extreme dimensions and inclinations, a contactless measurement method is selected to evaluate the angularity of overhangs. A FaroArm Edge with a laser line probe is used to capture the contour in the form of a point cloud. The angularity of downward faces of the overhang structures are then acquired by analyzing the point cloud with the 3D metrology software—PolyWorks. To be consistent about the measurement method, the configuration of measurement indicated here is used throughout this research, for both angularity of overhangs and cylindricity of holes.

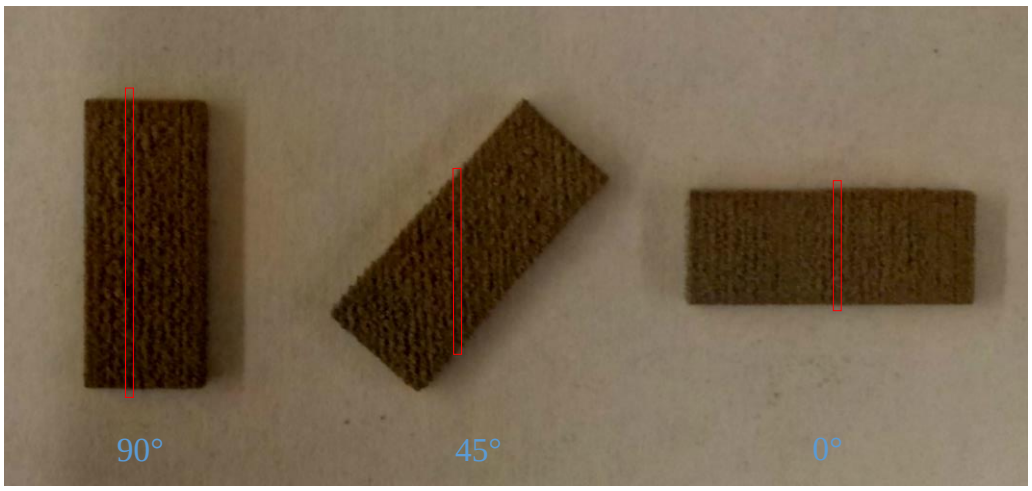

Figure 16 Image of strip texture on parts fabricated along different directions

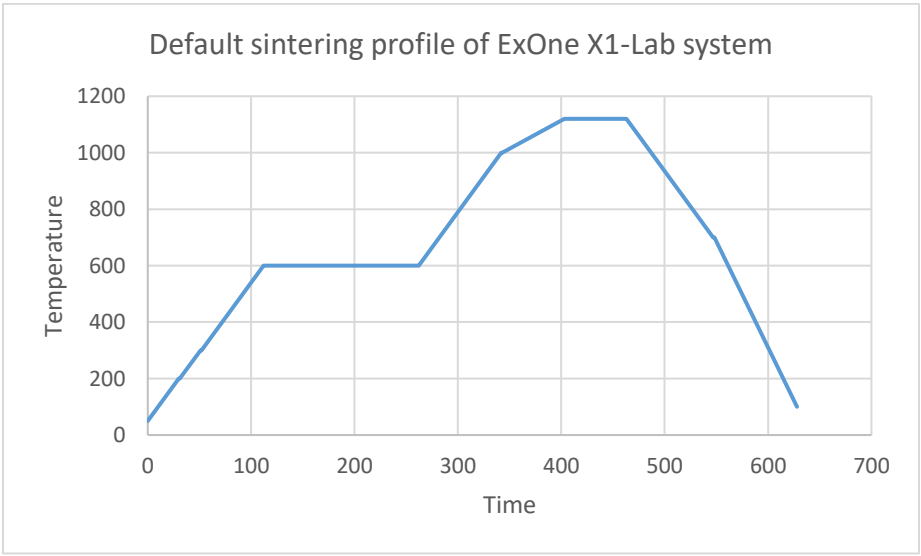

Figure 17. Default sintering profile of ExOne X1-Lab system

Table 3. Mechanical test results of standard test samples at different inclination angles

Mechanical test results / Inclination angle	Maximum stress (MPa)	
	Compression test	Tensile test
0°	107.6	6.5
45°	85.3	13.1
90°	99.8	20.2

3.2.1.2 Screening experiments of overhang structures

In this section, definitive screening design (DSD) is used to screen out the less important manufacturability parameters among the length, width, thickness and two inclination angles of the

overhang structures. The DSD platform in JMP DoE platforms is used to construct experimental runs and analyze the results. Powerful and convenient tools such as the Color Map on Correlations and Effective Model Selection for DSDs enable simple and clear demonstration of correlations among effects and unbiased identification of main effects and second-order effects.

For overhang structures, a DSD of 13 runs in 3 blocks is generated using JMP, as shown in Table 4. The ranges of manufacturability parameters and the number of block are selected based on the limited build volume of ExOne X1-Lab, as well as the symmetry of the overhang samples in terms of five manufacturability parameters. The Color Map of DSD for overhang structures shown in Figure 18 indicates the absolute correlations between effects with the reference color bar showing on the right. Red cells are only on the main diagonal so none of the effects are completely confounded with other effects. Most of all, main effects are uncorrelated with all two-way interaction because cells on the left and up sides are all blue cells.

Table 4. Definitive screening design for overhang structures

	Length	Thickness	Width	Inclination angle α	Inclination angle β	Angularity
1	17	5	20	90	30	0.196
2	17	0.6	4	0	90	0.449
3	26	2.8	4	90	30	0.316
4	8	2.8	20	0	90	0.254
5	26	0.6	12	0	30	1.235
6	8	5	12	90	90	0.065
7	26	5	4	45	90	0.307
8	8	0.6	20	45	30	0.325
9	26	5	20	0	60	0.926
10	8	0.6	4	90	60	0.356
11	26	0.6	20	90	90	0.211
12	8	5	4	0	30	0.196
13	17	2.8	12	45	60	0.436

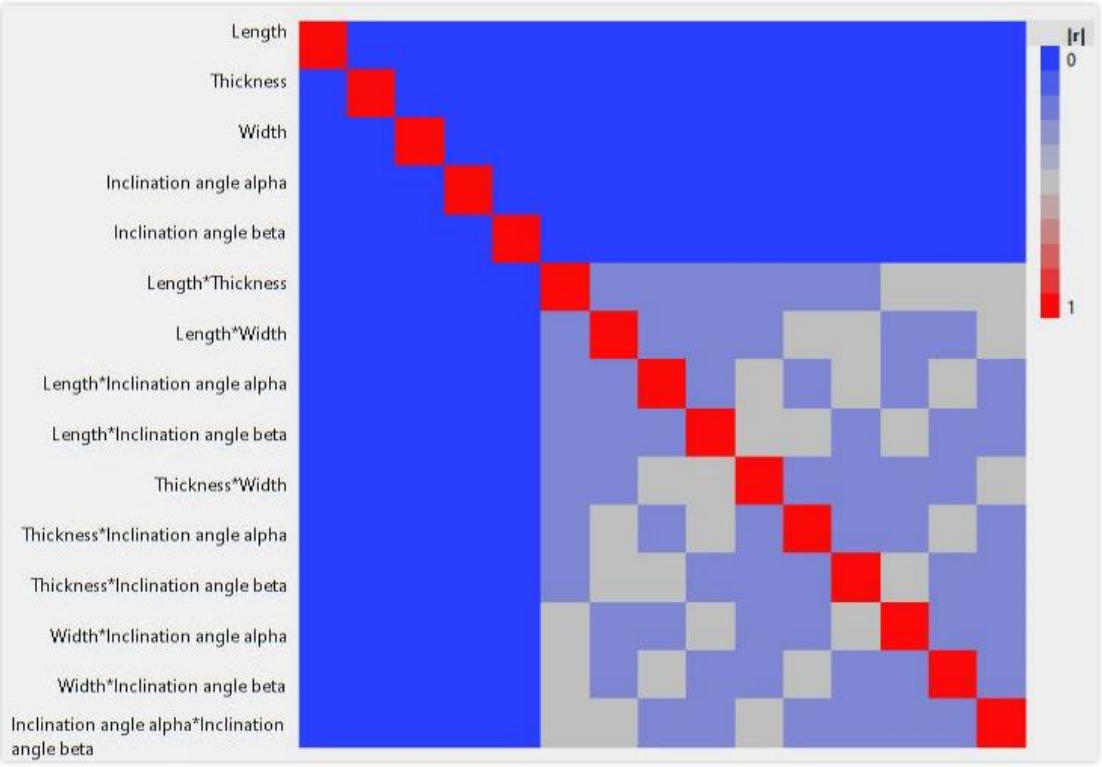

Figure 18. Color Map of Correlations of DSD for overhang structures

The measurement results of angularity are listed in Table 4. The contrast report and half normal report are generated with JMP to analyze the relative importance of five manufacturability parameters on the angularity and identify potential interactions between them. The contrast report shows relative importance of influence of independent variables on the response. The bar chart shows the t-ratio with blue line marking the threshold significance value. The critical value is determined by JMP. It is generous in its selection so that those that are possibly active are not missed. The factor whose t-ratio exceeds the critical significance value is the important factor that should be highlighted. The individual p-value and the simultaneous p-value are analogous to the standard p-values for a linear model, where small values of this value indicate a significant effect.

Term	Contrast		Lenth t-Ratio	Individual p-Value	Simultaneous p-Value
Inclination angle alpha	-0.168044		-4.13	0.0090*	0.0632
Length	0.157783		3.88	0.0112*	0.0793
Inclination angle beta	-0.086127		-2.12	0.0505	0.3509
Thickness	-0.077707		-1.91	0.0693	0.4623
Width	0.025259		0.62	0.5597	1.0000
Inclination angle alpha*Inclination angle alpha	0.027133		0.67	0.5081	1.0000
Inclination angle alpha*Length	-0.157383		-3.87	0.0113*	0.0799
Length*Length	0.021333	*	0.52	0.6293	1.0000
Inclination angle alpha*Inclination angle beta	-0.001323	*	-0.03	0.9738	1.0000
Length*Inclination angle beta	-0.039085	*	-0.96	0.3034	0.9932
Inclination angle beta*Inclination angle beta	-0.033382	*	-0.82	0.3768	0.9998
Inclination angle alpha*Inclination angle alpha*Length	-0.023417	*	-0.58	0.5957	1.0000

Figure 19. Contrast report of DSD for overhang structure

The Half Normal Plot in Figure 20 shows the absolute value of the contrasts against the normal quantiles for the absolute value normal distribution. Significant effects appear separated from the line towards the upper right of the graph. Four out of five design parameters have t-ratio larger than the threshold significance value, therefore are of importance: length, thickness, inclination angle α and β. Besides, there is a strong interaction between length and inclination angle α, which implies that the Taguchi method is not suitable for the final DoE of overhang structures.

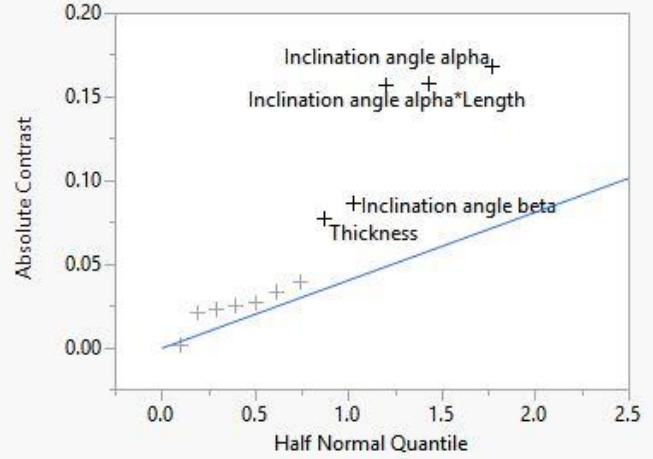

Figure 20. Half normal plot of DSD for overhang structure

3.2.1.3 Final experiments on overhang structures

Experiment data of four key manufacturability parameters and the corresponding angularity results are collected in the final experiments. Due to the factor interaction detected in the screening experiments and the lack of patterns that indicate the suitability of any specific fractional factorial

DoE method, the Custom Design platform in JMP is used to construct designs that fit a wide variety of settings. It is more cost effective and flexible than classical designs by offering many options that can be tailored for specific needs. For the final DoE, a custom design of 24 runs in 3 blocks is generated as shown in Table 5. The angularity of overhang samples is measured using the same measurement setting as used in screening experiments. The results are listed in Table 5. The experimental results listed here are used to build the manufacturability model for feature evaluation in the CADE system.

Table 5. Custom design for overhang structure

	Thickness	Length	Inclination angle α	Inclination angle β	Angularity
1	5	15	90	0	0.111
2	0.4	15	45	45	0.228
3	2.7	15	90	90	0.130
4	2.7	26	45	90	0.107
5	5	26	0	0	0.736
6	5	4	45	45	0.078
7	2.7	4	0	90	0.145
8	0.4	4	0	0	0.175
9	0.4	4	45	90	0.096
10	2.7	15	45	45	0.460
11	5	15	45	90	0.138
12	2.7	15	0	45	0.445
13	0.4	26	0	0	1.800
14	2.7	4	90	0	0.051
15	5	26	90	45	0.248
16	0.4	26	90	90	0.516
17	5	4	0	0	0.191
18	5	4	90	90	0.112
19	2.7	15	45	0	0.303
20	2.7	26	45	45	0.827
21	5	26	0	90	0.613
22	0.4	15	0	90	0.615
23	0.4	26	90	0	0.744
24	0.4	4	90	45	0.105

3.2.2 Through holes

In the mechanical designs, through holes are commonly used, and most likely, are required to fulfill some functionalities. The absence of material is normally reserved for other components like shafts to go through. The cylindrical surface usually provides support for the shaft in this case. The internal surface of holes is a type of common functional surface whose manufacturability is crucial for overall part quality. Besides, quality of additively manufactured holes is normally worse than the traditional counterparts in terms of surface roughness and cylindricity. The manufacturability of through holes is very important for the AM feature manufacturability.

The overhang structure is studied thoroughly in Section 3.2.1 to demonstrate each part of the DoE methodology and the CADE framework proposed in Chapter 2, whereas the experiment work of through hole is relatively brief to mitigate the workload of this research. A set of through holes with different diameters are manufactured in the preliminary experiments. The results show that through holes can be manufactured as small as 0.5 mm in diameter without any blockage. It is pointless to further decease the diameter smaller than 0.5 mm because the appropriate measurement methods would be limited and the scale of the dimension of features in this research is not intended to be that small. Therefore, through holes are redeemed as the manufacturable feature for the BJAM process.

Similar to the angularity of overhang structures, cylindricity is the form tolerance that is the most appropriate measure of manufacturability of through holes. The cylindricity is studied with respect to the key manufacturability parameters: diameter, inclination angles α and β. Given the scanning resolution and scanning accuracy of the FaroArm Edge and the build volume of ExOne X1-Lab system, the range of each key manufacturability parameters is determined and a custom design of 18 runs in 2 blocks is generated in JMP, as listed in Table 6. The contrast report in Figure 21 and

the half normal plot in Figure 22 indicate that the diameter is the key manufacturability parameter that affects the cylindricity of through holes, as well as the interactions between the diameter and the inclination angles α and β. Experimental data in Table 6 is used to develop the manufacturability model for feature evaluation.

Table 6. Custom design of through holes

	Diameter	Inclination angle α	Inclination angle β	Cylindricity
1	4	80	0	0.071
2	4	0	80	0.126
3	20	80	80	0.316
4	12	0	40	0.151
5	4	40	40	0.158
6	20	0	0	0.250
7	20	40	40	0.200
8	12	40	80	0.150
9	12	80	40	0.173
10	12	40	80	0.148
11	12	40	0	0.150
12	4	40	40	0.160
13	4	80	80	0.105
14	20	80	0	0.196
15	12	80	40	0.172
16	4	0	0	0.116
17	20	0	40	0.181
18	20	0	80	0.195

Term	Contrast		Lenth t-Ratio	Individual p-Value	Simultaneous p-Value
Diameter	0.040961		6.96	0.0008*	0.0047*
Inclination angle beta	0.006365		1.08	0.2601	0.9905
Inclination angle alpha	0.004381		0.74	0.4346	1.0000
Diameter*Diameter	0.008719	*	1.48	0.1372	0.8512
Diameter*Inclination angle beta	0.001750	*	0.30	0.7842	1.0000
Inclination angle beta*Inclination angle beta	-0.004341	*	-0.74	0.4381	1.0000
Diameter*Inclination angle alpha	0.014018	*	2.38	0.0330*	0.3076
Inclination angle beta*Inclination angle alpha	0.016583	*	2.82	0.0199*	0.2113
Inclination angle alpha*Inclination angle alpha	-0.001643	*	-0.28	0.7978	1.0000
Diameter*Diameter*Inclination angle beta	0.005272	*	0.90	0.3490	0.9998
Diameter*Inclination angle beta*Inclination angle beta	0.017576	*	2.99	0.0167*	0.1773
Diameter*Diameter*Inclination angle alpha	-0.003502	*	-0.60	0.5870	1.0000
Diameter*Inclination angle beta*Inclination angle alpha	0.012583	*	2.14	0.0475*	0.4273
Inclination angle beta*Inclination angle beta*Inclination angle alpha	-0.000749	*	-0.13	0.9051	1.0000

Figure 21. Contrast report of through hole

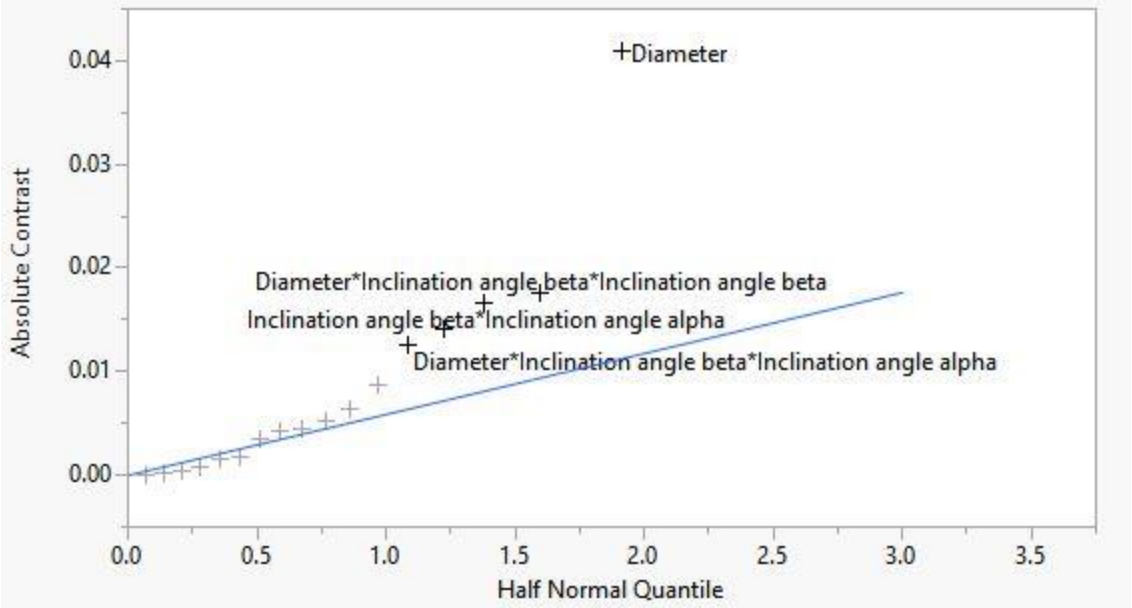

Figure 22. Half normal plot for through hole

3.3 Implementation of CADE system

3.3.1 Feature detection

Feature detection of CAD models is a complicated research work due to recognition difficulties imposed by feature intersection[69], ambiguous definition of various features in the feature knowledge base, complicated recognition algorithms, etc. In this research, a simplified pragmatic feature detection module is developed for the detection of overhang and hole structures. The feature detection logic is illustrated in the following sections and the feature detection module is then developed on the 3D modeling platform of Rhino3D and its graphical algorithm editor—Grasshopper. Grasshopper is a graphical programming platform for algorithm design in the CAD software—Rhino3D. Many build-in components can be used to process a variety of types of model data to extract information. Programming customized components for specific needs is available with Python, C# and C++.

3.3.1.1 Overhang structures

To build on the experiment work, the detection logic is developed for the typical overhang structures shown in Figure 15. In this thesis, the typical overhang structure is defined as a protruding structure whose shape is defined by five boundary planes with one of them facing downward. The downward-facing plane is called the overhang face, whose z-coordinate of the normal vector is negative. Based on this definition, the detection logic for overhang structure is proposed as shown in Figure 23 and developed with Grasshopper in Rhino.

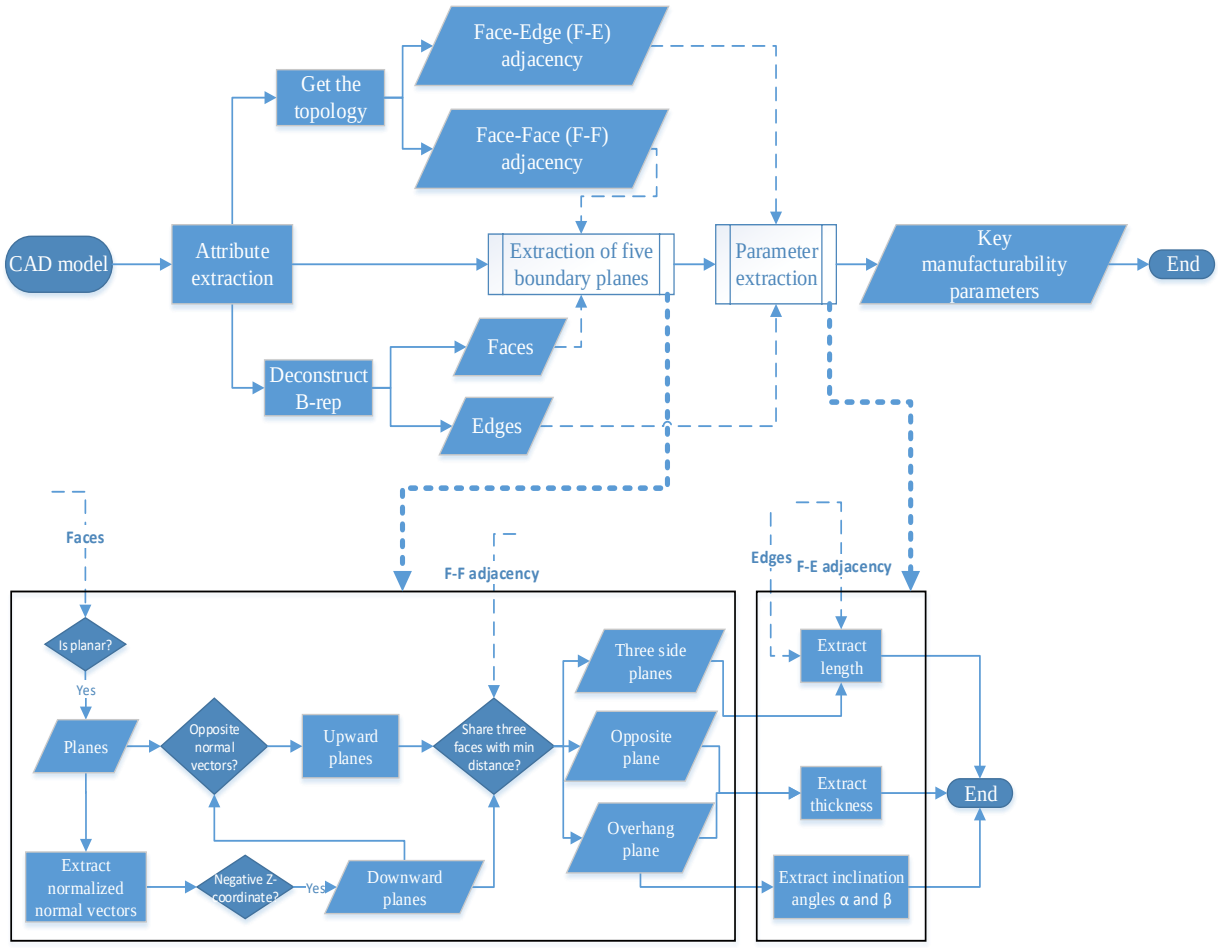

Figure 23. Flowchart of detection logic for overhang structure

The CAD model in the format of STEP file is deconstructed into attributes of faces, edges and topology relation of their adjacencies. Then in the first subprocess, the five boundary planes that

construct the overhang region (the overhang face and the opposite face and three side faces) are filtered from the extracted attributes through the following procedures: (1) find the downward faces that are planes with negative z-coordinate; (2) find the corresponding upward faces that are also planes whose normal vectors are opposite to the downward planes; (3) find the opposite plane that has the minimum distance to each downward plane among all upward planes and examine the number of shared faces between them: if they share three faces, the downward plane is deemed to be an overhang plane and these five planes comprise an overhang structure. The next subprocess is to extract the four key manufacturability parameters: length, thickness, inclination angles α and β. Two side planes that have opposite normal vectors among all three side planes are detected first. Two edges that are shared by one of the two opposite side planes with the overhang plane and the opposite plane respectively, are detected as well. The length of the shorter edge is the length of overhang structure. The distance between the opposite plane and the overhang plane is the thickness of overhang structure. The inclination angles α and β can be easily calculated by the normal vector of the overhang plane. The four manufacturability parameters are exported whose values are used as the input for feature evaluation. The graphical programming of the detection logic for overhang structure in Grasshopper is shown in Figure 24 and the Python code of the main components for detection is attached in the Appendix A.

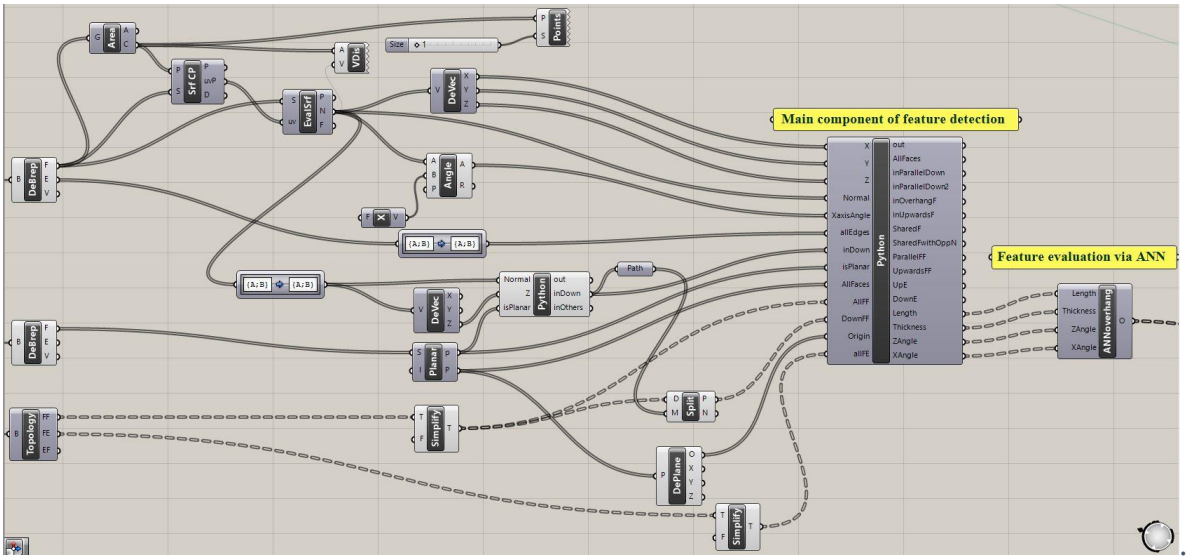

Figure 24. Graphical programming for the detection of overhang structure in Grasshopper

3.3.1.2 Through holes

The decision logic of detection for through hole is much simpler than that of overhang structure. The cylinder surface is extracted first. Two end circles are then identified as the shared edges between the cylinder surface and the adjacent planes. The diameter of through hole is extracted from the diameter of the end circles. The inclination angles of through hole are calculated from the inclination angles of the vector generated by two center points of the end circles, given that the domain of angles must be acute. The graphical programming of the detection logic for through hole in Grasshopper is shown in Figure 25 and the Python code of the main components for detection is attached in Appendix B.

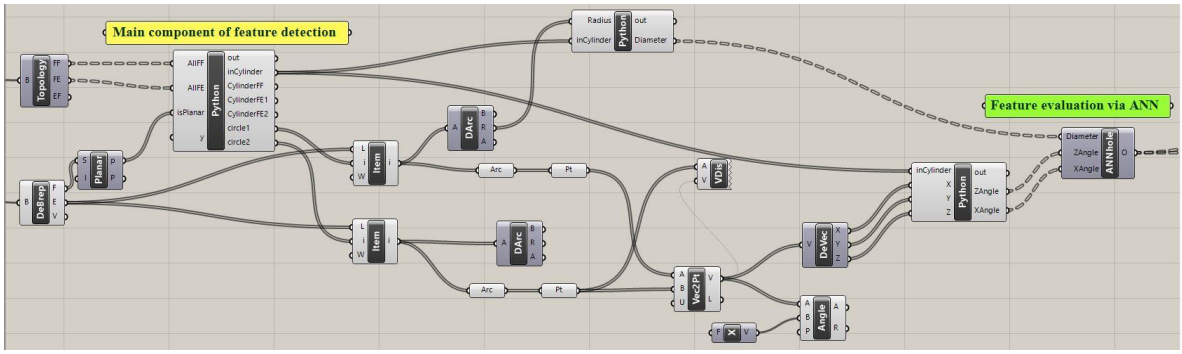

Figure 25. Graphical programming for the detection of through hole in Grasshopper

3.3.2 Feature evaluation and orientation optimization

There are mainly two types problems that ANN deals with: the supervised learning that is used to provide specified answer of outputs, and the unsupervised learning that is used to find the structures and patterns in datasets. The prediction of evaluation results is supposed to be continuous or discrete values, where regression model and classification model of supervised learning algorithms should be applied, respectively. In this research, a multiclass-classification algorithm of supervised learning is used to train the ANN. The structure of the ANN used in this research is a typical three-layer ANN, as shown in Figure 26.

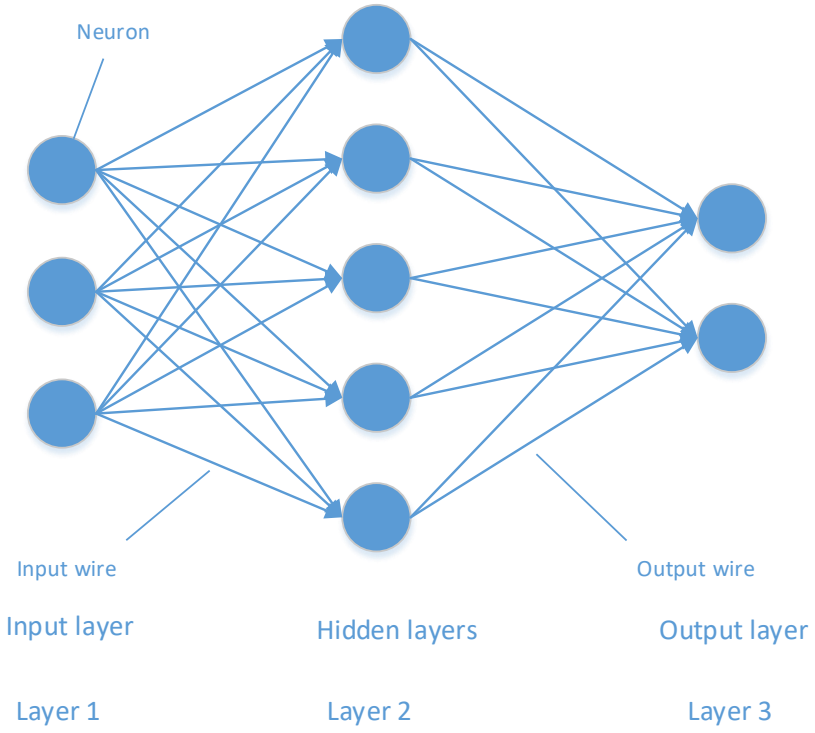

Figure 26. Structure of a typical three-layer ANN

ANN mimics the way that human brain transfers and processes information by artificially constructing several layers of logistic units called 'neurons' between the input units and output units. In Figure 26, the nodes or neurons between consecutive layers are connected by input/output

wires which represent the assigned weights of the neurons in one layer that are going to be counted in the next layer. The sigmoid activation function as shown in equation (8), also known as the hypothesis function, is widely used to calculate neurons in the next layer to carry the information forward up until the last output layer:

$$h_\theta(x) = \frac{1}{1+e^{-\theta^T x}} \tag{8}$$

Where x is the input vector, θ is the weight vector and $h_\theta(x)$ is the probability that the estimation is true given x parameterized by θ. The aforementioned process is called 'forward propagation' (FP). During the training of ANN, the squared difference between the calculated hypothesis output and the exact output is calculated, also known as the squared error term. This error term indicated how close the hypothesis output is to the exact output, which intuitively should be minimized by the backpropagation (BP) algorithm for a good fitting.

To utilize the one-vs-all multiclass classification scheme, the measurement data of angularity in Table 5 and cylindricity in Table 6 is discretized into integer numbers of grades. The values are rounded up to 0.01 and multiplied by 100. For example, the measured value of angularity is 0.111 for the first overhang sample, so the angularity grade of this overhang sample is 11. The processed datasets are used to train the ANNs for overhang structure and through hole using MATLAB codes programmed by the author. The MATLAB code includes FP and BP algorithms and fine tuning techniques of regularization and gradient checking. The program code of ANN for overhang structure is attached in the Appendix C, whereas that of the through hole is similar thus not repeated again here. The training accuracy of ANNs for overhang structure and through hole are 91.30% and 88.89% respectively. Given the experimental condition available for this research, the training accuracies are reasonable. Due to the small build volume of BJAM system used for experiments and the relatively complicated process procedure of BJAM, only a limited number of samples can

be printed in each experiment run and the number of experiment samples that is affordable for this research is limited. To ensure the necessary quantity of training data for ANN, the experiment runs are divided into several blocks, which introduces more variations and uncertainties in the data acquirement for ANN. The training accuracy can be improved if more experimental data can be gathered for training the ANN.

The manufacturability model is established by the trained ANN, which is not an explicitly derived expression of the objective/fitness function for optimization. The trained ANN is used as a black box. Inputs (key manufacturability parameters of corresponding features) are fed in the ANN to get the evaluation results. The trained ANN is used to evaluate an aerospace bracket case study in Chapter 4.

The feature detection module is implemented in Grasshopper whereas the ANN is programmed and trained using MATLAB. Speaking from the point view of software implementation, the feature detection module and the feature evaluation module cannot interact with each other directly because of compatibility issues. Comparing all the available choices, it is most convenient to program a specialized component using C# in Grasshopper that can call the trained ANN, rather than program GA codes in MATLAB and then configure the interaction between Grasshopper and MATLAB in the computer system level. The C# program code of the specialized component is attached in the Appendix D. The adjustment of build orientation is implemented in Grasshopper, as shown in Figure 27. Orientation optimization is conducted by the GA optimization solver add-on components in Grasshopper—Galapogas. Weighted-sum method is used to evaluate both the angularity of overhang structures and the cylindricity of through holes of the CAD model.

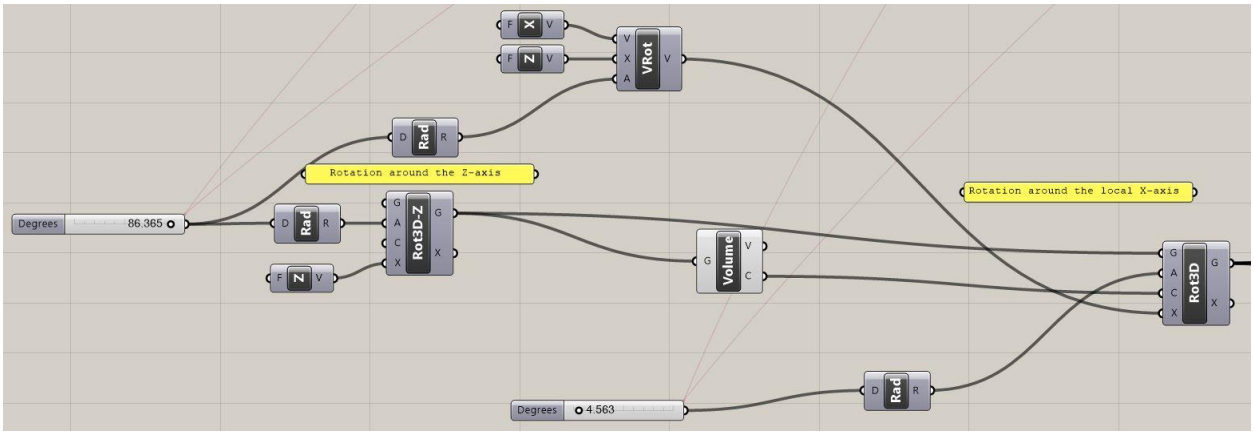

Figure 27. Graphical programming of adjustment of build orientation

3.4 Summary

In this chapter, the CADE system proposed in Chapter 2 is implemented for the BJAM process. Extensive experimental work is conducted to study the manufacturability of the BJAM process. Based on the knowledge and experiment data gained, the CADE system is then developed. The CADE system is mainly implemented in the graphical programming platform—Grasshopper. A logic rule-based feature detection module for STEP file format is developed by using Grasshopper build-in components and specialized components programmed using Python. A specialized component programmed with C# is also developed to call the trained ANN for feature evaluation. The GA optimization solver add-on components in Grasshopper—Galapogas is used in the orientation optimization module. The training accuracies of overhang structure and through hole are 91.30% and 88.89% respectively. The decent training accuracies indicate a good performance of the trained ANN, given the small number of training data gained from time-consuming experiment runs and limited measurement accuracy of laser scanning device. To prove the effectiveness of the developed ANN, a case study of an aerospace engineering bracket is evaluated by the developed CADE system with respect to its overall manufacturability in the next chapter.

4 Case study

An aerospace engineering bracket is used as the case study to validate the feasibility of the developed CADE system. This bracket part is assembled in a dynamic assembly system and the company that provides this reference part would like to know how the part is going to be designed for three metal AM processes (including the BJAM process) and the manufacturability of the redesigned part for the specific metal AM processes. Due to confidentiality of this project, the details of the original and redesigned parts cannot be revealed in this thesis. Therefore, only the design envelope of the bracket part is shown in Figure 28 and is used as the reference part to conduct the case study.

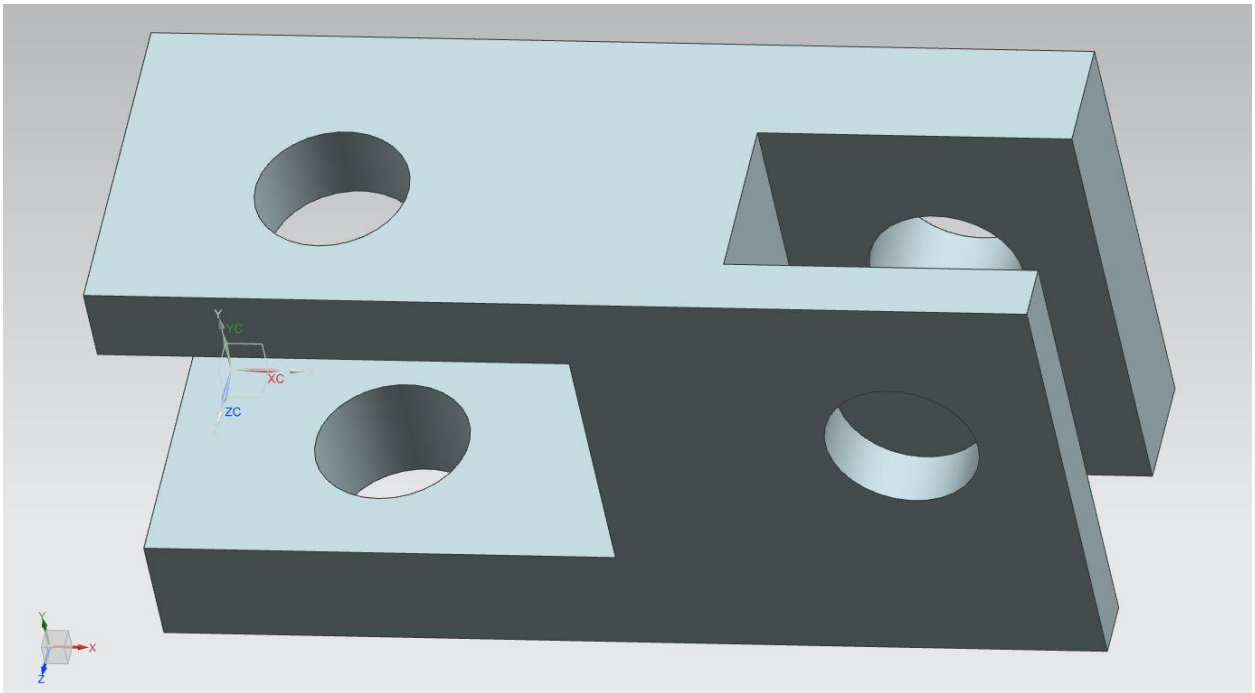

Figure 28. Reference part for case study

This reference part is a perfect example of the trade-off that is required in manufacturability analysis. It consists of four overhang structures with through holes in the overhang regions that stick out both horizontally and perpendicularly. The diameter of the four through holes is the same,

but thickness and length of the overhang structures are different. In the developed CADE system, the overall manufacturability of the whole part is the weighted sum of the angularity of overhang structures and the cylindricity of through holes. The weight coefficients reflect the relative importance of manufacturability of through holes and overhang structures in this part, which should be determined by the designer based on the design requirements. The change of build orientation of the part itself will result in the change of all the design features in it. The weighted sum value is then optimized with respect to the build orientation of the part.

Three sets of weight coefficients are selected to evaluate the reference part with the developed CADE system. The overall manufacturability of the part is optimized and listed as the prediction results in Table 7. The angularity and cylindricity are discretized grade values as illustrated in Chapter 3, thus, the value of prediction result is the weighted sum of corresponding angularity grades and cylindricity grades. The same apparatus, methods, material and parameters that are used to study the manufacturability of BJAM process and acquire experiment data for developing the CADE system as listed in Table 1 and shown in Figure 17, are used to manufacture the optimized reference parts.

Table 7. Comparison of predicted and measured results of the reference part

Weight coefficient		Evaluation result	Measurement result in average	Relative error
Overhang	Hole			
0.3	0.7	9.2	9.7	5%
0.5	0.5	8.0	8.6	8%
0.7	0.3	6.8	7.4	9%

For each set of weight coefficients, three parts are manufactured and measured. The average measurement results are listed in Table 7. The relative errors between the measured results of as-manufactured parts and the evaluated results of as-design models are below 10% for all three cases, which indicate that the developed CADE system is capable of providing reliable manufacturability analysis of the specific BJAM process.

5 Conclusions

Additive manufacturing (AM) is a state-of-the-art manufacturing technique that is tremendously changing the ways products are designed, manufactured and delivered. AM is well-known for its capability of manufacturing complex shapes and intricate features, however, due to its inherent additive way of manufacturing parts layer by layer, AM is subjected to some unique manufacturing constraints that need to be considered in the design stage.

To provide practitioners with knowledges of the designated AM process, most researchers and equipment suppliers propose feature-based design guidelines for practitioners. On one hand, the design guidelines usually connect the AM feature manufacturability to only one manufacturability parameter so that they are simple to follow. On the other hand, they can be too general to represent the dependent relation between the manufacturability of features and their corresponding manufacturability parameters. To compensate for the shortcoming of the design guidelines, manufacturability analysis is employed to examine the features in specified designs for potential manufacturing failures. In this presented work, a computer-aided design evaluation (CADE) system is proposed to perform manufacturability analysis of designs for specific AM processes. This feature-based software tool is developed in an experimental way. The proposed three-stage DoE method systematically investigates the manufacturability of the designated AM process. The evaluation criteria and key manufacturability parameters are identified and the experimental data are collected.

The CADE system consists of three modules: feature detection, feature evaluation and orientation optimization. Features and key manufacturability parameters in the design model are identified and extracted in the feature detection module. With the support of well-designed experiments, the feature evaluation module establishes the model of dependent relation between the key

manufacturability parameters and the manufacturability of the corresponding feature, that is 'the manufacturability model', via artificial neural network (ANN). Due to the importance and the complexity of build orientation of AM parts, the orientation optimization module then optimizes overall manufacturability of the part with respect to the build orientation by using genetic algorithm (GA). The optimization result indicates the best overall manufacturability result of the designed part, which helps designers to identify the problematic design features in advance of the manufacturing stage.

The proposed CADE system is implemented in the context of BJAM process. Overhang structures and through holes are selected as the research objects due to their well-known low manufacturability in AM processes. The three-stage experiments are conducted and the CADE system is developed on the 3D modeling platform of Rhino3D and its graphical algorithm editor—Grasshopper. For the experimentation work, it is found that BJAM not only suffers from the anisotropic effect in the printing direction as any other AM processes do, but are also subjected to the anisotropic effect in the direction in which the binder droplets are applied. Angularity and cylindricity are used as the evaluation criteria of overhang structures and through holes, respectively. Key manufacturability parameters that play the most important roles are identified in the preliminary experiments. It is determined that length, thickness and two inclination angles are key parameters for overhang structures, whereas diameter and two inclination angles are key parameters for through holes. As for the software development work, the feature detection and orientation optimization modules are graphically programmed in Grasshopper and the feature evaluation module is developed in MATLAB. The case study of an engineering bracket is performed and the evaluation results are accurate for the manufacturability analysis of BJAM

process. The developed CADE system evaluates the manufacturability of AM parts before manufacturing takes place, which can reduce the risk of manufacturing failures.

More features should be studied experimentally so that the CADE system can be developed for evaluating more complex parts in the future. Besides, the experimental results acquired in this study might be biased due to the limited build volume of the BJAM apparatus used. Future work should also include the implementation of the proposed CADE system in a bigger build volume where the dimension of experiment parts is not limited.

Reference

[1] Yang, F., Tang, Y., and Zhao, Y. F., 2016, "Manufacturability of Overhang Structures Fabricated by Binder Jetting Process," (50527), p. V002T002A063.
[2] Conner, B. P., Manogharan, G. P., Martof, A. N., Rodomsky, L. M., Rodomsky, C. M., Jordan, D. C., and Limperos, J. W., 2014, "Making sense of 3-D printing: Creating a map of additive manufacturing products and services," Additive Manufacturing, 1–4, pp. 64-76.
[3] Gao, W., Zhang, Y., Ramanujan, D., Ramani, K., Chen, Y., Williams, C. B., Wang, C. C. L., Shin, Y. C., Zhang, S., and Zavattieri, P. D., 2015, "The status, challenges, and future of additive manufacturing in engineering," CAD Computer Aided Design, 69, pp. 65-89.
[4] Yang, S., Tang, Y., and Zhao, Y. F., 2015, "A new part consolidation method to embrace the design freedom of additive manufacturing," Journal of Manufacturing Processes, 20, Part 3, pp. 444-449.
[5] Bourell, D., Beaman, J., Marcus, H., and Barlow, J., "Solid freeform fabrication an advanced manufacturing approach," Proc. Proceedings of the SFF Symposium, pp. 1-7.
[6] Goguelin, S., Flynn, J. M., and Dhokia, V., 2016, "A Bottom-up Design Framework for CAD Tools to Support Design for Additive Manufacturing," Sustainable Design and Manufacturing 2016, R. Setchi, R. J. Howlett, Y. Liu, and P. Theobald, eds., Springer International Publishing, Cham, pp. 411-421.
[7] Ranjan, R., Samant, R., and Anand, S., "Design for manufacturability in additive manufacturing using a graph based approach," Proc. ASME 2015 International Manufacturing Science and Engineering Conference, MSEC 2015, June 8, 2015 - June 12, 2015, American Society of Mechanical Engineers, p. Manufacturing Engineering Division.
[8] Nelaturi, S., Arvind, W. K., and Kurtoglu, R. T., "Manufacturability feedback and model correction for additive manufacturing," Proc. ASME 2014 International Design Engineering Technical Conferences and Computers and Information in Engineering Conference, IDETC/CIE 2014, August 17, 2014 - August 20, 2014, American Society of Mechanical Engineers (ASME), p. Computers and Information in Engineering Division; Design Engineering Division.
[9] Vayre, B., Vignat, F., and Villeneuve, F., 2012, "Designing for additive manufacturing," Procedia CIrP, 3, pp. 632-637.
[10] Atzeni, E., and Salmi, A., 2015, "Study on unsupported overhangs of AlSi10Mg parts processed by Direct Metal Laser Sintering (DMLS)," Journal of Manufacturing Processes, 20, pp. 500-506.
[11] Cheng, B., and Chou, K., 2015, "Geometric consideration of support structures in part overhang fabrications by electron beam additive manufacturing," CAD Computer Aided Design, 69, pp. 102-111.
[12] Samperi, M. T., 2014, "Development of Design Guidelines for Metal Additive Manufacturing and Process Selection," The Pennsylvania State University.
[13] Thomas, D., 2009, "The development of design rules for selective laser melting," University of Wales.
[14] Kumke, M., Watschke, H., and Vietor, T., 2016, "A new methodological framework for design for additive manufacturing," Virtual and Physical Prototyping, 11(1), pp. 3-19.
[15] Laverne, F., Segonds, F., Anwer, N., and Le Coq, M., 2015, "Assembly Based Methods to Support Product Innovation in Design for Additive Manufacturing: An Exploratory Case Study," Journal of Mechanical Design, 137(12), pp. 121701-121701-121708.
[16] Seepersad, C. C., Govett, T., Kim, K., Lundin, M., and Pinero, D., "A Designer's Guide for Dimensioning and Tolerancing SLS parts," Proc. 23rd Annual International Solid Freeform Fabrication Symposium, Austin, TX, pp. 921-931.
[17] Seepersad, C. C., "Design Rules and Detail Resolution for SLS 3D Printing."
[18] Meisel, N., and Williams, C., 2015, "An Investigation of Key Design for Additive Manufacturing Constraints in Multimaterial Three-Dimensional Printing," Journal of Mechanical Design, 137(11), p. 111406.

[19] Salonitis, K., 2016, "Design for additive manufacturing based on the axiomatic design method," Int J Adv Manuf Technol, 87(1), pp. 989-996.
[20] Chen, H., and Zhao, Y. F., 2016, "Process parameters optimization for improving surface quality and manufacturing accuracy of binder jetting additive manufacturing process," Rapid Prototyping Journal, 22(3), pp. 527-538.
[21] Klahn, C., Leutenecker, B., and Meboldt, M., 2014, "Design for Additive Manufacturing – Supporting the Substitution of Components in Series Products," Procedia CIRP, 21, pp. 138-143.
[22] Kerbrat, O., Mognol, P., and Hascoet, J. Y., 2010, "Manufacturability analysis to combine additive and subtractive processes," Rapid Prototyping Journal, 16(1), pp. 63-72.
[23] Zhang, Y., Bernard, A., Gupta, R. K., and Harik, R., 2014, "Evaluating the design for additive manufacturing: a process planning perspective," Procedia CIRP, 21, pp. 144-150.
[24] Maidin, S. B., Campbell, I., and Pei, E., 2012, "Development of a design feature database to support design for additive manufacturing," Assembly Automation, 32(3), pp. 235-244.
[25] Kruth, J.-P., Vandenbroucke, B., Vaerenbergh, v. J., and Mercelis, P., 2005, "Benchmarking of different SLS/SLM processes as rapid manufacturing techniques."
[26] Gao, J., Zheng, D. T., Gindy, N., and Clark, D., 2005, "Extraction/conversion of geometric dimensions and tolerances for machining features," Int J Adv Manuf Technol, 26(4), pp. 405-414.
[27] Babic, B., Nesic, N., and Miljkovic, Z., 2008, "A review of automated feature recognition with rule-based pattern recognition," Computers in Industry, 59(4), pp. 321-337.
[28] Bhandarkar, M. P., and Nagi, R., 2000, "STEP-based feature extraction from STEP geometry for Agile Manufacturing," Computers in Industry, 41(1), pp. 3-24.
[29] JungHyun, H., and Requicha, A. A. G., 1998, "Feature recognition from CAD models," IEEE Computer Graphics and Applications, 18(2), pp. 80-94.
[30] Zehtaban, L., and Roller, D., 2016, "Automated Rule-based System for Opitz Feature Recognition and Code Generation from STEP," Computer-Aided Design and Applications, 13(3), pp. 309-319.
[31] Garg, A., Tai, K., and Savalani, M., 2014, "State-of-the-art in empirical modelling of rapid prototyping processes," Rapid Prototyping Journal, 20(2), pp. 164-178.
[32] Negi, S., and Sharma, R. K., 2016, "Study on shrinkage behaviour of laser sintered PA 3200GF specimens using RSM and ANN," Rapid Prototyping Journal, 22(4), pp. 645-659.
[33] Badkar, D. S., Pandey, K. S., and Buvanashekaran, G., 2013, "Development of RSM- and ANN-based models to predict and analyze the effects of process parameters of laser-hardened commercially pure titanium on heat input and tensile strength," Int J Adv Manuf Technol, 65(9), pp. 1319-1338.
[34] Munguía, J., Ciurana, J., and Riba, C., 2009, "Neural-network-based model for build-time estimation in selective laser sintering," Proceedings of the Institution of Mechanical Engineers, Part B: Journal of Engineering Manufacture, 223(8), pp. 995-1003.
[35] Rong-Ji, W., Xin-hua, L., Qing-ding, W., and Lingling, W., 2009, "Optimizing process parameters for selective laser sintering based on neural network and genetic algorithm," Int J Adv Manuf Technol, 42(11), pp. 1035-1042.
[36] Peng, A., Xiao, X., and Yue, R., 2014, "Process parameter optimization for fused deposition modeling using response surface methodology combined with fuzzy inference system," Int J Adv Manuf Technol, 73(1), pp. 87-100.
[37] Cong-Zhong, C., Jun-Fang, P., Yu-Feng, W., Xing-Jian, Z., and Ting-Ting, X., 2009, "Density prediction of selective laser sintering parts based on support vector regression," Acta Physica Sinica, 58(Suppl 1), pp. 8-13.
[38] Bacchewar, P., Singhal, S., and Pandey, P., 2007, "Statistical modelling and optimization of surface roughness in the selective laser sintering process," Proceedings of the Institution of Mechanical Engineers, Part B: Journal of Engineering Manufacture, 221(1), pp. 35-52.

[39] Beal, V., Paggi, R., Salmoria, G., and Lago, A., 2009, "Statistical evaluation of laser energy density effect on mechanical properties of polyamide parts manufactured by selective laser sintering," Journal of Applied Polymer Science, 113(5), pp. 2910-2919.
[40] Kruth, J. P., and Kumar, S., 2005, "Statistical analysis of experimental parameters in selective laser sintering," Advanced Engineering Materials, 7(8), pp. 750-755.
[41] Desai, K. M., Survase, S. A., Saudagar, P. S., Lele, S. S., and Singhal, R. S., 2008, "Comparison of artificial neural network (ANN) and response surface methodology (RSM) in fermentation media optimization: Case study of fermentative production of scleroglucan," Biochemical Engineering Journal, 41(3), pp. 266-273.
[42] Kleijnen, J. P. C., 2015, "Response Surface Methodology," Handbook of Simulation Optimization, M. C. Fu, ed., Springer New York, New York, NY, pp. 81-104.
[43] Desai, K. M., Vaidya, B. K., Singhal, R. S., and Bhagwat, S. S., 2005, "Use of an artificial neural network in modeling yeast biomass and yield of β-glucan," Process Biochemistry, 40(5), pp. 1617-1626.
[44] Ebrahimpour, A., Rahman, R. N. Z. R. A., Ean Ch'ng, D. H., Basri, M., and Salleh, A. B., 2008, "A modeling study by response surface methodology and artificial neural network on culture parameters optimization for thermostable lipase production from a newly isolated thermophilic Geobacillus sp. strain ARM," BMC Biotechnology, 8, pp. 96-96.
[45] Erzurumlu, T., and Oktem, H., 2007, "Comparison of response surface model with neural network in determining the surface quality of moulded parts," Mater. Des., 28(2), pp. 459-465.
[46] Pilkington, J. L., Preston, C., and Gomes, R. L., 2014, "Comparison of response surface methodology (RSM) and artificial neural networks (ANN) towards efficient extraction of artemisinin from Artemisia annua," Industrial Crops and Products, 58, pp. 15-24.
[47] Basri, M., Rahman, R. N. Z. R. A., Ebrahimpour, A., Salleh, A. B., Gunawan, E. R., and Rahman, M. B. A., 2007, "Comparison of estimation capabilities of response surface methodology (RSM) with artificial neural network (ANN) in lipase-catalyzed synthesis of palm-based wax ester," BMC Biotechnology, 7(1), p. 53.
[48] Prakash Maran, J., Sivakumar, V., Thirugnanasambandham, K., and Sridhar, R., 2013, "Artificial neural network and response surface methodology modeling in mass transfer parameters predictions during osmotic dehydration of Carica papaya L," Alexandria Engineering Journal, 52(3), pp. 507-516.
[49] Azzahari, A., Yusuf, S., Selvanathan, V., and Yahya, R., 2016, "Artificial Neural Network and Response Surface Methodology Modeling in Ionic Conductivity Predictions of Phthaloylchitosan-Based Gel Polymer Electrolyte," Polymers, 8(2), p. 22.
[50] Li, X. f., Dong, J. h., and Zhang, Y. z., "Modeling and Applying of RBF Neural Network Based on Fuzzy Clustering and Pseudo-Inverse Method," Proc. 2009 International Conference on Information Engineering and Computer Science, pp. 1-4.
[51] Equbal, A., Sood, A. K., and Mahapatra, S., 2010, "Prediction of dimensional accuracy in fused deposition modelling: a fuzzy logic approach," International Journal of Productivity and Quality Management, 7(1), pp. 22-43.
[52] Lee, S., Park, W., Cho, H., Zhang, W., and Leu, M.-C., 2001, "A neural network approach to the modelling and analysis of stereolithography processes," Proceedings of the Institution of Mechanical Engineers, Part B: Journal of Engineering Manufacture, 215(12), pp. 1719-1733.
[53] Luo, Z., Yang, F., Dong, G., Tang, Y., and Zhao, Y. F., 2016, "Orientation Optimization in Layer-Based Additive Manufacturing Process," (50077), p. V01AT02A039.
[54] Renner, G., and Ekárt, A., 2003, "Genetic algorithms in computer aided design," Computer-Aided Design, 35(8), pp. 709-726.
[55] Canellidis, V., Giannatsis, J., and Dedoussis, V., 2009, "Genetic-algorithm-based multi-objective optimization of the build orientation in stereolithography," International Journal of Advanced Manufacturing Technology, 45(7-8), pp. 714-730.

[56] Hur, S. M., Choi, K. H., Lee, S. H., and Chang, P. K., 2001, "Determination of fabricating orientation and packing in SLS process," Journal of Materials Processing Technology, 112(2-3), pp. 236-243.
[57] Antony, J., 2003, Design of Experiments for Engineers and Scientists.
[58] Dougherty, S., Simpson, J. R., Hill, R. R., Pignatiello, J. J., and White, E. D., 2015, "Nonlinear screening designs for defense testing: an overview and case study," The Journal of Defense Modeling and Simulation, 12(3), pp. 335-342.
[59] Wass, J. A., 2010, "First Steps in Experimental Design-The Screening Experiment," Journal of Validation Technology, 16(2), p. 49.
[60] Jones, B., and Nachtsheim, C. J., 2011, "A Class of Three-Level Designs for Definitive Screening in the Presence of Second-Order Effects," J. Qual. Technol., 43(1), pp. 1-15.
[61] Errore, A., Jones, B., Li, W., and Nachtsheim, C. J., 2017, "Using Definitive Screening Designs to Identify Active First- and Second-Order Factor Effects," J. Qual. Technol., 49(3), pp. 244-264.
[62] Khaw, J. F. C., Lim, B. S., and Lim, L. E. N., 1995, "Optimal design of neural networks using the Taguchi method," Neurocomputing, 7(3), pp. 225-245.
[63] Altan, M., 2010, "Reducing shrinkage in injection moldings via the Taguchi, ANOVA and neural network methods," Mater. Des., 31(1), pp. 599-604.
[64] Ko, D.-C., Kim, D.-H., and Kim, B.-M., 1999, "Application of artificial neural network and Taguchi method to preform design in metal forming considering workability," International Journal of Machine Tools and Manufacture, 39(5), pp. 771-785.
[65] Jinn-Tsong, T., Jyh-Horng, C., and Tung-Kuan, L., 2006, "Tuning the structure and parameters of a neural network by using hybrid Taguchi-genetic algorithm," IEEE Transactions on Neural Networks, 17(1), pp. 69-80.
[66] Utela, B., Storti, D., Anderson, R., and Ganter, M., 2008, "A review of process development steps for new material systems in three dimensional printing (3DP)," Journal of Manufacturing Processes, 10(2), pp. 96-104.
[67] Allen, S., and Sachs, E., 2000, "Three-dimensional printing of metal parts for tooling and other applications," Metals and Materials, 6(6), pp. 589-594.
[68] ExOne, "ExOne digital part materialization," http://exone.com/en/materialization/solutions.
[69] Han, J., 1996, "3d geometric reasoning algorithms for feature recognition," University of Southern California.

Appendix

Appendix A. Python code for the detection of overhang structure

```
# Import GH core library to use DataTree in Python
import rhinoscriptsyntax as rs
import clr
clr.AddReference("Grasshopper")
import Grasshopper.Kernel.Data.GH_Path as ghpath
import Grasshopper.DataTree as datatree
import System
import math

#----------------------------inParallelDown--------------------------------

inParallelDown = datatree[System.Object]()
Tol = 0.0001

#find the index of faces that are planes and in parallel with the downwards planes
for i in range(len(inDown)):
    path = ghpath(inDown[i])
    for j in range(len(Normal)):
        if rs.VectorLength(Normal[inDown[i]] + Normal[j]) < Tol and abs(isPlanar[j] - 1)
< Tol:
            inParallelDown.Add(j,path)

#-------------------------------ParallelFF---------------------------------

tree = datatree[System.Object]()

for i in range(inParallelDown.BranchCount):
    for j in range(len(inParallelDown.Branch(i))):
        path = ghpath(inParallelDown.Branch(i)[j])
        if path in tree.Paths:
          continue
        else: tree.Add(AllFF.Branch(inParallelDown.Branch(i)[j]),path)
ParallelFF = tree

#----------------------inOverhang, Upwards, SharedF-------------------------

# To create a tree of sharedF between downwards planes (as shown in the tree path)
# and corresponding parallel faces, check if EXACTLY 3 faces are shared, i.e. found the
upwards faces
inOverhangF = []
inParallelDown2 = datatree[System.Object]()
UpwardsFF = datatree[System.Object]()
SharedF = datatree[System.Object]()
for i in range(DownFF.BranchCount): #the i-th branch of the DownFF tree
    path1 = ghpath(DownFF.Path(i)) #store index of downward plane in path1
#    print path1
    for m in range(len(inParallelDown.Branch(i))): #m-th parallel plane to the i-th
downwards plane
        count = 0
        for j in range(len(DownFF.Branch(i))):
            for n in range(len(AllFF.Branch(inParallelDown.Branch(i)[m]))): # the n-th
item of the m-th parallel tree
```

```
                if AllFF.Branch(inParallelDown.Branch(i)[m])[n] == DownFF.Branch(i)[j]
and isPlanar[DownFF.Branch(i)[j]] == 1: #i-th DownFF tree and  FF-tree of it's m-th
parallel plane share a same face index, which must be a plane itself
                    count = count + 1
#        print count
        if count == 3:
            if inDown[i] not in inOverhangF:
                inOverhangF.append(inDown[i])
            inParallelDown2.Add(inParallelDown.Branch(i)[m],path1)
            continue

#-------------------------------------Thickness-----------------------------

inUpwardsF = datatree[System.Object]()
# find the minDistance between overhang planes and all upwards planes (stored in the
inUpwardsF tree),
# as well as store the indices of planes with minDis(thickness) in the tree of inUpwardsF
Thickness = datatree[System.Object]()
for i in range(len(inOverhangF)):
    lst = []
    for j in range(len(inParallelDown2.Branch(i))):

lst.append(abs(AllFaces[inParallelDown2.Branch(i)[j]].DistanceTo(Origin[inOverhangF[i]]))
)
    Min = min(lst)
#    print Min
    path = ghpath(inOverhangF[i])
    inUpwardsF.Add(inParallelDown2.Branch(i)[lst.index(Min)],path)
    Thickness.Add(Min,path)

#-----------SharedF between the overhang plane and its upwards plane---------

for i in range(len(inOverhangF)):
    path = ghpath(inOverhangF[i])
    for m in range(len(inUpwardsF.Branch(i))):
        for j in range(len(AllFF.Branch(inOverhangF[i]))):
            for n in range(len(AllFF.Branch(inUpwardsF.Branch(i)[m]))):
                if AllFF.Branch(inUpwardsF.Branch(i)[m])[n] ==
AllFF.Branch(inOverhangF[i])[j] and isPlanar[AllFF.Branch(inOverhangF[i])[j]] == 1:
                    SharedF.Add(AllFF.Branch(inOverhangF[i])[j],path)

# get the shared faces that have opposite normals to each other within each branch of the
'SharedF' tree, which is determined as the shared faces that points to the 'overhang
direction'
tree = datatree[System.Object]()
Tol = 0.0001
for l in range(SharedF.BranchCount):
    for m in range(len(SharedF.Branch(l))):
        if m == len(SharedF.Branch(l))-1:
            break
        for n in range(len(SharedF.Branch(l))-m-1):
            if rs.VectorLength(Normal[SharedF.Branch(l)[m]] +
Normal[SharedF.Branch(l)[m+n+1]]) < Tol and abs(isPlanar[SharedF.Branch(l)[m]] - 1) < Tol
and abs(isPlanar[SharedF.Branch(l)[m+n+1]] - 1) < Tol:
                path = ghpath(SharedF.Path(l))
                tree.Add(SharedF.Branch(l)[m],path)
                tree.Add(SharedF.Branch(l)[m+n+1],path)
SharedFwithOppN = tree
```

```
#get shared edges between the shared face and downwards face as well as upwards face
respectively,
#the shared edge with smaller length among those two is the length of overhang structure
#meaning the overhangs must be squared on the sides so that side edges points along the
'overhang direction'

#get shared edges between the shared face and downwards face
DownE = datatree[System.Object]()
for i in range(SharedFwithOppN.BranchCount):
    for j in range(len(allFE.Branch(SharedFwithOppN.Path(i)))):
        for k in range(len(allFE.Branch(SharedFwithOppN.Branch(i)[0]))): #within the edge
list of one of (the first, hence the [0]) shared face
#            print allFE.Branch(SharedFwithOppN.Branch(i)[0])
            if allFE.Branch(SharedFwithOppN.Path(i))[j] ==
allFE.Branch(SharedFwithOppN.Branch(i)[0])[k]:
#                print allFE.Branch(SharedFwithOppN.Branch(i)[0])
                path = ghpath(SharedFwithOppN.Path(i))
                length =
rs.CurveLength(allEdges[allFE.Branch(SharedFwithOppN.Path(i))[j]])
                DownE.Add(allFE.Branch(SharedFwithOppN.Path(i))[j], path) #first, append
the edge index
                DownE.Add(length, path)                                    #then, append
the length of this edge

#get shared edges between the shared face and upwards face
UpE = datatree[System.Object]()
for i in range(SharedFwithOppN.BranchCount):
    for j in range(len(allFE.Branch(inUpwardsF.Branch(i)[0]))):
        for k in range(len(allFE.Branch(SharedFwithOppN.Branch(i)[0]))): #within the edge
list of one of (the first, hence the [0]) shared face

            if allFE.Branch(inUpwardsF.Branch(i)[0])[j] ==
allFE.Branch(SharedFwithOppN.Branch(i)[0])[k]:

                path = ghpath(SharedFwithOppN.Path(i))
                length =
rs.CurveLength(allEdges[allFE.Branch(inUpwardsF.Branch(i)[0])[j]])
                UpE.Add(allFE.Branch(inUpwardsF.Branch(i)[0])[j], path) #first, append
the edge index
                UpE.Add(length, path)                                    #then, append the
length of this edge

Length = datatree[System.Object]()
for i in range(DownE.BranchCount):
    l = min(DownE.Branch(i)[1],UpE.Branch(i)[1])
    path = ghpath(DownE.Path(i))
Length.Add(l,path)

#-------------------------Angle w.r.t X-axis and Z-axis----------------------

# given the symmetry of overhang features due to the combination of theta-X and theta-Z,
# the angle range is cut down to [0,90] respectively in the experiments, and the angles
is calculated basedc on the symmetry as well
import math
Tol = 1e-4

XAngle = datatree[System.Object]()
```

```
ZAngle = datatree[System.Object]()
for i in range(len(inOverhangF)):
    path = ghpath(inOverhangF[i])
    a1 = XaxisAngle[SharedFwithOppN.Branch(i)[0]]

ZAngle.Add(180/math.pi*min(XaxisAngle[SharedFwithOppN.Branch(i)[0]],XaxisAngle[SharedFwit
hOppN.Branch(i)[1]]),path)
#since only Z-axis and local X-axis rotations allowed and the overhang structure is
squared, Z-rotation angle w.r.t X-axis is always the smaller angle among the angles
between Shared side planes and X-axis
XAngle.Add(90-
abs(180/math.pi*math.atan(Z[inOverhangF[i]]/math.sqrt(X[inOverhangF[i]]**2+Y[inOverhangF[
i]]**2))), path)
```

Appendix B. Python code for the detection of through hole

```
# Import GH core library to use DataTree in Python
import rhinoscriptsyntax as rs
import clr
clr.AddReference("Grasshopper")
import Grasshopper.Kernel.Data.GH_Path as ghpath
import Grasshopper.DataTree as datatree
import System
import math

inCylinder = list()
CylinderFF = datatree[System.Object]()
CylinderFE1 = datatree[System.Object]()
CylinderFE2 = datatree[System.Object]()
for i in range(AllFF.BranchCount):
    if isPlanar[i] == 0:
        inCylinder.append(i)
        path = ghpath(i)
#        print AllFF.Branch(i)
        for j in range(len(AllFF.Branch(i))):
            CylinderFF.Add(AllFF.Branch(i)[j],path)

for m in range(len(inCylinder)):
    path = ghpath(inCylinder[m])
    for i in range(len(AllFE.Branch(CylinderFF.Branch(m)[0]))):
        for k in range(len(AllFE.Branch(inCylinder[m]))):
            if AllFE.Branch(CylinderFF.Branch(m)[0])[i] ==
AllFE.Branch(inCylinder[m])[k]:
                CylinderFE1.Add(AllFE.Branch(inCylinder[m])[k],path)\

#--------------------extraction of two end circles---------------------------
circle1 = list()
for i in range(len(inCylinder)):
    circle1.append(CylinderFE1.Branch(i)[0])

for m in range(len(inCylinder)):
    path = ghpath(inCylinder[m])
    for j in range(len(AllFE.Branch(CylinderFF.Branch(m)[1]))):
        for k in range(len(AllFE.Branch(inCylinder[m]))):
            if AllFE.Branch(CylinderFF.Branch(m)[1])[j] ==
AllFE.Branch(inCylinder[m])[k]:
                CylinderFE2.Add(AllFE.Branch(inCylinder[m])[k],path)
```

```
circle2 = list()
for i in range(len(inCylinder)):
circle2.append(CylinderFE2.Branch(i)[0])
```

Appendix C. MATLAB code of ANN training for the overhang structure

```
%% Initialization
clear ; close all; clc

%% Setup the parameters you will use for this exercise
% Load Training Data
fprintf('Loading Traning Data ...\n')

load('dataOverhang.mat');
m = size(x, 1);

input_layer_size  = size(x, 2);  % the number of features (design parameters)
hidden_layer_size = 20;   % 10 hidden units
% NEED TO BE CHANGED
output_layer_size = 83;          % Labels of quality performance (the range of all
measure value;
                                 % penalize the failed parts with a very large label)

%% ================ Part 1: Initializing Parameters ================
%  Implment a two layer neural network that classifies quality performances.
%  Start by implementing a function to initialize the weights of the neural
%  network(randInitializeWeights.m)

fprintf('\nInitializing Neural Network Parameters ...\n')

initial_Theta1 = randInitializeWeights(input_layer_size, hidden_layer_size);
initial_Theta2 = randInitializeWeights(hidden_layer_size, output_layer_size);

% Unroll parameters
initial_nn_params = [initial_Theta1(:) ; initial_Theta2(:)];

%% ================ Part 2: Compute Cost (Feedforward) ================
%  For the neural network, you should first start by implementing the
%  feedforward part of the neural network that returns the cost only.
%
%  Suggestion: implement the feedforward cost *without* regularization
%  first so that it will be easier for you to debug. Later, in part 3, you
%  will get to implement the regularized cost.
%
fprintf('\nFeedforward Using Neural Network ...\n')

% Weight regularization parameter (set this to 0 here).
lambda = 0;

J = nnCostFunction(initial_nn_params, input_layer_size, hidden_layer_size, ...
                   output_layer_size, x, Y, lambda);

fprintf('Cost at initial parameters: %f ', J);

fprintf('\nProgram paused. Press enter to continue.\n');
pause;
```

```
%% =============== Part 3: Implement Regularization ===============
%

fprintf('\nChecking Cost Function (w/ Regularization) ... \n')

% Weight regularization parameter (we set this to 1 here).
lambda = 1;

J = nnCostFunction(initial_nn_params, input_layer_size, hidden_layer_size, ...
                   output_layer_size, x, Y, lambda);

fprintf('Cost at initial parameters (with regularization): %f ', J);

fprintf('Program paused. Press enter to continue.\n');
pause;
%% =============== Part 4: Implement Backpropagation ===============
%  Add to the code in nnCostFunction.m to return the partial derivatives of the
parameters.
%
fprintf('\nChecking Backpropagation... \n');

%  Check gradients by running checkNNGradients
checkNNGradients;

fprintf('\nProgram paused. Press enter to continue.\n');
pause;


%% =============== Part 5: Implement Regularization ===============
%
%  continue to implement the regularization with the cost and gradient.
%

fprintf('\nChecking Backpropagation (with Regularization) ... \n')

%  Check gradients by running checkNNGradients
lambda = 1;
checkNNGradients(lambda);

fprintf('Program paused. Press enter to continue.\n');
pause;


%% ================== Part 6: Training NN ==================
% To train the neural network, we will now use "fmincg", which
%  is a function which works similarly to "fminunc". Recall that these
%  advanced optimizers are able to train our cost functions efficiently as
%  long as we provide them with the gradient computations.
%
fprintf('\nTraining Neural Network... \n')

%  Change the MaxIter to a larger value to see how more training helps.
options = optimset('MaxIter', 5000);

%  You should also try different values of lambda
lambda = 0;

% Create "short hand" for the cost function to be minimized
```

```
costFunction = @(p) nnCostFunction(p, ...
                                   input_layer_size, ...
                                   hidden_layer_size, ...
                                   output_layer_size, x, Y, lambda);

% Now, costFunction is a function that takes in only one argument (the
% neural network parameters)
[nn_params, cost] = fmincg(costFunction, initial_nn_params, options);


% Obtain Theta1 and Theta2 back from nn_params
Theta1 = reshape(nn_params(1:hidden_layer_size * (input_layer_size + 1)), ...
                 hidden_layer_size, (input_layer_size + 1));

Theta2 = reshape(nn_params((1 + (hidden_layer_size * (input_layer_size + 1))):end), ...
                 output_layer_size, (hidden_layer_size + 1));

fprintf('Program paused. Press enter to continue.\n');
pause;

save('ThetaOverhang.mat','Theta1','Theta2')


%% ================ Part 7: Implement Predict ================
%  After training the neural network, we would like to use it to predict
%  the labels. You will now implement the "predict" function to use the
%  neural network to predict the labels of the training set. This lets
%  you compute the training set accuracy.

pred = predict(Theta1, Theta2, x);

fprintf('\nTraining Set Accuracy: %f\n', mean(double(pred == Y)) * 100);
```

Appendix D. C# code of specialized Grasshopper component for overhang structure

```
using System;
using System.Collections.Generic;

using Grasshopper.Kernel;
using Rhino.Geometry;

namespace ANN
{
    public class ANNComponent : GH_Component
    {
        /// <summary>
        /// Each implementation of GH_Component must provide a public
        /// constructor without any arguments.
        /// Category represents the Tab in which the component will appear,
        /// Subcategory the panel. If you use non-existing tab or panel names,
        /// new tabs/panels will automatically be created.
        /// </summary>
        public ANNComponent()
```

```
            : base("ANNoverhang", "ANNoverhang",
                "PredictOverhangAngularity",
                "ANNoverhang", "ANNoverhang")
        {
        }

        /// <summary>
        /// Registers all the input parameters for this component.
        /// </summary>
        protected override void RegisterInputParams(GH_Component.GH_InputParamManager
pManager)
        {
            pManager.AddNumberParameter("Length", "Length", "length",
GH_ParamAccess.item);
            pManager.AddNumberParameter("Thickness", "Thickness", "Thickness",
GH_ParamAccess.item);
            pManager.AddNumberParameter("ZAngle", "ZAngle", "ZAngle",
GH_ParamAccess.item);
            pManager.AddNumberParameter("XAngle", "XAngle", "XAngle",
GH_ParamAccess.item);


        }

        /// <summary>
        /// Registers all the output parameters for this component.
        /// </summary>
        protected override void RegisterOutputParams(GH_Component.GH_OutputParamManager
pManager)
        {
            pManager.AddNumberParameter("OutPut","O","output",GH_ParamAccess.item);
        }

        /// <summary>
        /// This is the method that actually does the work.
        /// </summary>
        /// <param name="DA">The DA object can be used to retrieve data from input
parameters and
        /// to store data in output parameters.</param>
        protected override void SolveInstance(I44GH_DataAccess DA)
        {
            double length=0;
            double zangle=0;
            double xangle=0;
            if(!DA.GetData(0,ref length)||!DA.GetData(1,ref thickness)||!DA.GetData(2,ref
zangle)||!DA.GetData(3,ref xangle))
            {
                return;
            }
            MLApp.MLApp matlab = new MLApp.MLApp();
            double[] input = new double;

            // Change to the directory where the function is located
            matlab.Execute(@"cd C:\Users\Fan\OneDrive\McGill\Journal&Thesis\CADE");

            // Define the output
            object result = null;
```

```
            // Call the MATLAB function myfunc
            matlab.Feval("pre-overhang", 1, out result, input);

            // Display result
            object[] res = result as object[];

            double outputresult = (double) res[0];

            DA.SetData(0, outputresult);

            Console.WriteLine(res[0]);
            Console.ReadLine();
        }

        /// <summary>
        /// Provides an Icon for every component that will be visible in the User
Interface.
        /// Icons need to be 24x24 pixels.
        /// </summary>
        protected override System.Drawing.Bitmap Icon
        {
            get
            {
                // You can add image files to your project resources and access them like
this:
                //return Resources.IconForThisComponent;
                return null;
            }
        }

        /// <summary>
        /// Each component must have a unique Guid to identify it.
        /// It is vital this Guid doesn't change otherwise old ghx files
        /// that use the old ID will partially fail during loading.
        /// </summary>
        public override Guid ComponentGuid
        {
            get { return new Guid("{8cc80555-1000-4ec0-aa88-24e14bd679e7}"); }
        }
    }
}
```